



Review

Synthesis and catalytic utilization of bimetallic systems for wastewater remediation: A review

Khyle Glainmer N. Quiton ^a, Ming-Chun Lu ^{b,*}, Yao-Hui Huang ^{a,**}

^a Department of Chemical Engineering, Sustainable Environment Research Center, National Cheng Kung University, Tainan, 701, Taiwan

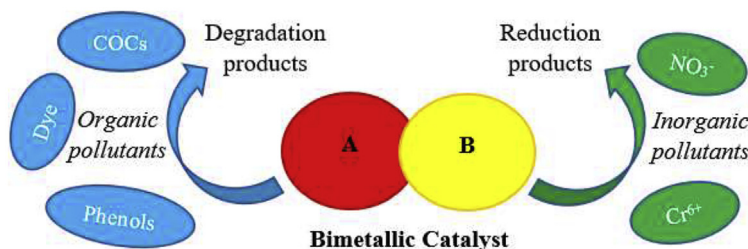
^b Department of Environmental Resources Management, Chia Nan University of Pharmacy and Science, Tainan, 71710, Taiwan



HIGHLIGHTS

- Bimetallic catalysts possess different physicochemical properties than those of monometallic catalysts.
- Bimetallic catalysts have remarkable catalytic properties and functions, and exhibit high reducibility.
- Organic and inorganic pollutants in water and wastewater can be treated using bimetallic systems.

GRAPHICAL ABSTRACT



ARTICLE INFO

Article history:

Received 26 May 2020

Received in revised form

2 September 2020

Accepted 15 September 2020

Available online 18 September 2020

Handling Editor: Tsair-Fuh

Keywords:

Bimetallic catalyst

Catalyst synthesis

Heterogeneous catalysts

Organic pollutants

Water treatment

Wastewater treatment

ABSTRACT

The environment is affected by agricultural, domestic, and industrial activities that lead to drastic problems such as global warming and wastewater generation. Wastewater pollution is of public concern, making the treatment of persistent pollutants in water and wastewater highly imperative. Several conventional treatment technologies (physicochemical processes, biological degradation, and oxidative processes) have been applied to water and wastewater remediation, but each has numerous limitations. To address this issue, treatment using bimetallic systems has been extensively studied. This study reviews existing research on various synthesis methods for the preparation of bimetallic catalysts and their catalytic application to the treatment of organic (dyes, phenol and its derivatives, and chlorinated organic compounds) and inorganic pollutants (nitrate and hexavalent chromium) from water and wastewater. The reaction mechanisms, removal efficiencies, operating conditions, and research progress are also presented. The results reveal that Fe-based bimetallic catalysts are one of the most efficient heterogeneous catalysts for the treatment of organic and inorganic contamination. Furthermore, the roles and performances of bimetallic catalysts in the removal of these environmental contaminants are different.

© 2020 Elsevier Ltd. All rights reserved.

Contents

1. Introduction	2
2. Unique properties of bimetallic catalysts	2
3. Synthesis methods	3
3.1. Co-precipitation	3

* Corresponding author.

** Corresponding author.

E-mail addresses: mmclu@mail.cnu.edu.tw (M.-C. Lu), yhuang@mail.ncku.edu.tw (Y.-H. Huang).

3.2.	Deposition precipitation	5
3.3.	Plasma spraying	5
3.4.	Impregnation	5
3.4.1.	Types of impregnation	5
3.4.2.	Impregnation methods	6
3.5.	Sol-gel method	6
3.6.	Reverse micelle method	6
4.	Catalytic application for contaminant remediation	7
4.1.	Treatment of organic pollutants	7
4.1.1.	Conventional treatment technologies	8
4.1.2.	Dye degradation	8
4.1.3.	Degradation of phenol and its derivatives	11
4.1.4.	Chlorinated organic compounds (COCs)	13
4.2.	Inorganic pollutant treatment	13
4.2.1.	Conventional treatment methods	13
4.2.2.	Nitrate reduction	14
4.2.3.	Hexavalent chromium reduction	15
5.	Remarks and conclusions	16
	Declaration of competing interest	17
	Acknowledgements	17
	References	17

1. Introduction

Environmental pollution is becoming increasingly severe. Many regions are heading towards a water crisis. According to the World Health Organization (WHO), water resource scarcity affects over 40% of the world's population, with 2 billion people having little to no access to clean water. The process of industrialization and urbanization has doubled global water utilization every 15 years. At present, water availability is a pressing concern. Additionally, water pollution caused by industrial and urban activities has led to increasing concentrations of various pollutants in natural waters, affecting human health and well-being (Fu et al., 2015, 2014).

Natural waters are usually the final destinations for wastewater containing various kinds of pollutant. The discharge of untreated wastewater results in the accumulation of persistent contaminants, including heavy metals and organic and inorganic compounds (Rodrigues et al., 2019). Thus, water remediation and wastewater treatment are of utmost importance.

In recent years, various physicochemical processes have been proposed for treating wastewaters, including those based on adsorption, chemical precipitation, coagulation/flocculation, filtration, ion exchange, and sedimentation. Biological degradation and conventional oxidative processes that involve the degradation of the pollutant in the presence of oxygen or other oxidants, such as hydrogen peroxide, ozone, and permanganate, have also been developed. However, physicochemical processes concentrate pollutants at another phase, which requires further treatment (or post-treatment). Similarly, although biological degradation is relatively inexpensive, the generated by-products are often highly toxic and non-biodegradable (Al-Khalid and El-Naas, 2012; Lavanya et al., 2014; Pandya et al., 2018). Conventional oxidative processes cannot completely oxidize refractory compounds with high chemical stability. Thus, intermediate products, which can be even more toxic than the original pollutants, are most likely to be formed during oxidation (Rodrigues et al., 2019).

To overcome the drawbacks of these processes, bimetallic catalysts have been extensively studied for the removal of a wide range of contaminants in wastewater remediation. The limitations of monometallic catalysts include slow contaminant removal efficiency, easy deactivation, and the sensitivity of removal efficiency to pH. To enhance the reactivity of catalysts, bimetallic catalysts

were developed by coating small amounts of a transition or noble metal onto a freshly prepared metal surface.

There has been a lot of interest in the synthesis and utilization of bimetallic catalysts for the removal of contaminants, especially from wastewater. Fig. 1 shows that the number of journal publications has increased in the period 2000–2018 for the keywords “bimetallic catalyst synthesis” and “bimetallic catalyst for wastewater remediation”.

Several studies reported on the remediation of different organic and inorganic contaminants in water and wastewater. However, there are hardly any papers reviewing their removal using bimetallic catalysts. In addition, no comprehensive study on the reaction mechanisms in the removal of these environmental pollutants using the said catalysts exists to date. Thus, the synthesis and use of bimetallic catalysts in the removal of environmental contaminants from water and wastewater are reviewed in this paper. This review focuses on synthesis methods for the preparation of bimetallic catalysts, the removal efficiency of pollutants, operating conditions, and reaction mechanisms of bimetallic catalysts for certain organic and inorganic pollutants.

This perspective hopes to give an overview of the past and recent research developed in this field, and steer future research to acquire optimal catalytic systems for environmental pollutant removal.

2. Unique properties of bimetallic catalysts

Catalysis on bimetallic alloys advanced over the past few decades. In the 1940s, bimetallic catalysts were studied due to their enhanced activity, selectivity, and stability resulting from the ensemble, electronic, and bifunctional effects between the two different metal components. When one of the surface components is catalytically inactive, ensemble effects usually take place. This surface component only acts to dilute the active metal component into discrete aggregates or ensembles of atoms. Moreover, smaller ensemble size is preferable because it permits only the desired reaction and prevents unwanted and non-selective reactions (Yuan et al., 2007).

The incorporation of a second metal into the catalyst may lead to modifications or changes in the geometric as well as the electronic characteristics of the catalyst. This results in the modification of the

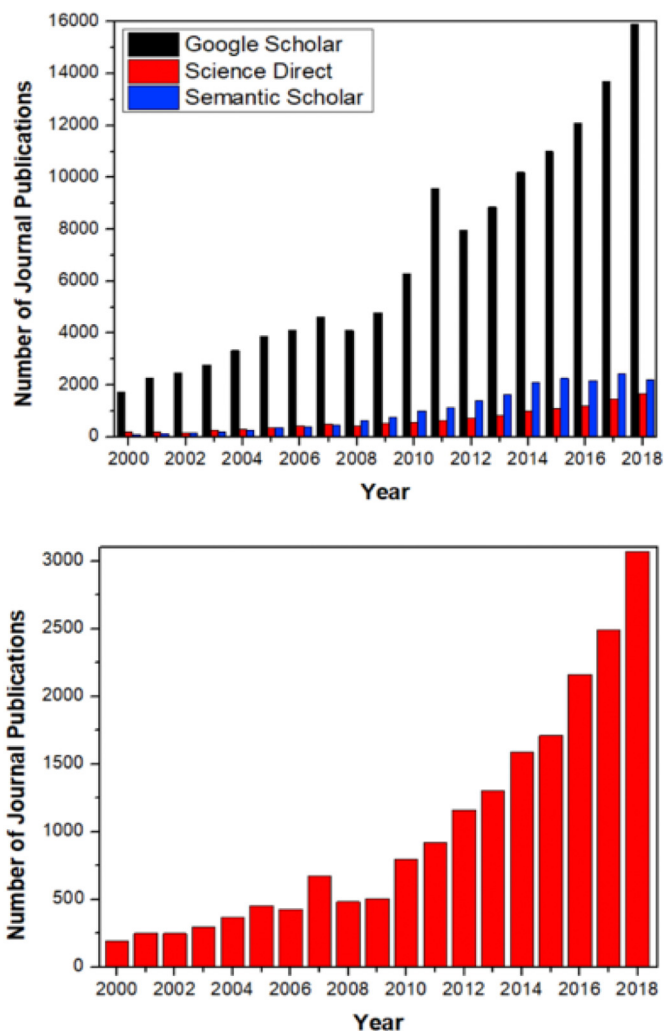


Fig. 1. Number of journals published from 2000 to 2018 with the keywords (a) "bimetallic catalyst synthesis" from three academic search engines and (b) "bimetallic catalyst for wastewater remediation" from Google Scholar.

adsorption characteristics of the bimetallic catalyst's surface and in some cases alters its reduction and deactivation behavior. Ali et al. revealed that bimetallic catalysts exhibit different physicochemical properties than those of monometallic catalysts (Ali et al., 2012).

Heterogeneous catalysis occurs on the catalyst surface. Therefore, the surface structure and chemistry of bimetallic catalysts in terms of the geometric and electronic structures of metal atoms on the surface are the most significant parameters. Similar to other chemical processes performed at the interface of two phases, heterogeneous catalysis is always performed at an interface of a solid catalyst and gaseous or liquid reactants around it (Tao et al., 2012).

The electronic and geometric effects result from the differences in catalytic behavior between different catalysts (including bimetallic catalysts, monometallic catalysts, and two bimetallic catalysts with different compositions and structures). The electronic effect (accompanying the formation of a geometrically favorable binding site) is also called the ligand effect (Liao et al., 2015).

3. Synthesis methods

There is a wide range of synthesis techniques for preparing supported bimetallic catalysts. This section provides a summary of some of the most common methods used for bimetallic catalyst

synthesis and the potential advantages and disadvantages of each method (Table 1).

The composition and catalytic performance of bimetallic catalysts are usually related to the catalyst preparation method. These factors include metal salt precursor and reaction environments (affected by temperature, pH, and pressure), active phase cost, catalyst surface area, and specific catalytic characteristics (Duvenhage and Coville, 2005). A slight change in these factors can alter the properties and performance of the catalysts. Only a few methods are used in the chemical industry due to the cost of the raw materials and limitations in terms of storage, transportation, and potential for large-scale production.

3.1. Co-precipitation

Precipitation may be caused by a change in certain parameters such as temperature, pH, evaporation, and/or concentration of metal salts. It has been extensively used to synthesize single-component catalysts or supported and mixed catalysts. Controlled precipitation from precursor solutions is governed by the principles of nucleation, in which the smallest stable elementary particles of the new phase form under specific precipitation conditions, and growth or the agglomeration of the particles (Deraz, 2018; Munnik et al., 2015). In co-precipitation, the solutions containing the active metal salt and a salt of a compound to be converted as the support are mixed with a base (NaOH, Na₂CO₃, etc.) to precipitate as hydroxides and/or carbonates for the single-step nucleation and growth of the combined solid precursor of the active metal and the catalyst support (Munnik et al., 2015; Pinna, 1998). It is one of the most convenient ways to produce bimetallic catalysts with a high metal weight-to-volume ratio, achieving a 70 wt% metal loading or even higher while maintaining small particle sizes (Munnik et al., 2015). In the precipitation method, the following reaction occurs:

Metal salt solution

+ support → metal hydroxide or carbonate on the support

(1)

Powders or particles are slurred with an amount of salt to sufficiently obtain the required loading. Hydroxides and carbonates are the preferred intermediates for the precipitation method for the following reasons (Perego and Villa, 1997):

- The solubility of the salts of transition metals is very low. This leads to very high supersaturations, resulting in very small precipitate particle sizes.
- Hydroxides and carbonates are easily decomposed via heat into oxides with relatively high areas without leaving potential catalyst poisons.
- The calcination of hydroxides and/or carbonates causes minimal safety and environmental problems.

In the co-precipitation method, utmost care must be taken to avoid independent or consecutive precipitations. In this case, the pH should be adjusted and kept constant during the operation by mixing the starting solution continuously instead of the addition of one solution to another. Fig. 2(a) shows the synthesis of supported bimetallic catalysts via the co-precipitation technique. A mixture of metal precursors is dissolved in a specific amount of ethanol and precipitated using Na₂CO₃ solution, or any hydroxide or carbonate. Then, the support precursor is added and mixed thoroughly until a homogeneous mixture is obtained. Consequently, the resulting precipitate may be washed, dried, and/or calcined to obtain the target metal components on the catalyst surface.

Table 1
Advantages and disadvantages of various synthesis methods for bimetallic catalysts.

Synthesis method	Advantages	Disadvantages	Reference
Co-precipitation	<ol style="list-style-type: none"> 1. Homogeneity of component distribution 2. Relatively low reaction temperature 3. Particle size is fine and uniform with weakly agglomerated particles 	<ol style="list-style-type: none"> 1. Insensitive 2. Semi-quantitative 3. Long reaction time 4. Consumes large quantities of chemicals 	Deraz (2018)
Deposition precipitation	<ol style="list-style-type: none"> 1. Easy control of particle size and composition 2. Various possibilities to modify the particle surface state and overall homogeneity 	<ol style="list-style-type: none"> 1. Trace impurities may precipitate with the product 2. Time-consuming 3. Does not work well if the reactants have very different precipitation rates 	Silas et al. (2018)
Plasma technique	<ol style="list-style-type: none"> 1. Shortened catalyst preparation time 2. Low energy requirements 3. Highly distributed active species are produced 4. Production of uniform metal particle size 5. Enhanced selectivity 6. Enhanced catalyst lifetime 	<ol style="list-style-type: none"> 1. Complex methods cannot be applied on industrial scale 2. Catalyst deactivation problem 	(Aluha et al., 2016; Aluha and Abatzoglou, 2017)
Impregnation	<ol style="list-style-type: none"> 1. Quick process 2. Inexpensive 3. Final properties and configuration can be easily controlled in advance 	<ol style="list-style-type: none"> 1. Difficult to prepare catalyst with high concentration 2. Difficult to obtain even dispersion of catalyst components on the support surface 3. Particles need calcination 	Deraz (2018)
Sol-gel method	<ol style="list-style-type: none"> 1. Superior homogeneity and purity 2. Good microstructural control of metallic particles 3. Large BET surface area 4. Good thermal stability of the supported metals 5. Additional elements can be added easily 6. Hydroxylation on the support is easy to control 7. Low crystallization temperature 	<ol style="list-style-type: none"> 1. Time-consuming 2. High maintenance and operation costs 3. Particles need calcination 	(Gonzalez et al., 1997; Taghavimoghaddam et al., 2012)
Reverse micelle method	<ol style="list-style-type: none"> 1. Narrow particle size distributions 2. Negligible contamination of the product during homogenization of starting compounds 3. Low energy consumption 4. Low aging times 5. Use of simple equipment 6. Improved control of particle sizes, shapes, uniformity, and dispersity 	<ol style="list-style-type: none"> 1. Difficult to separate particles from the constituents (e.g., surfactants) 2. Colloidal formation is a complex process 	Uskoković and Drofenik (2005)

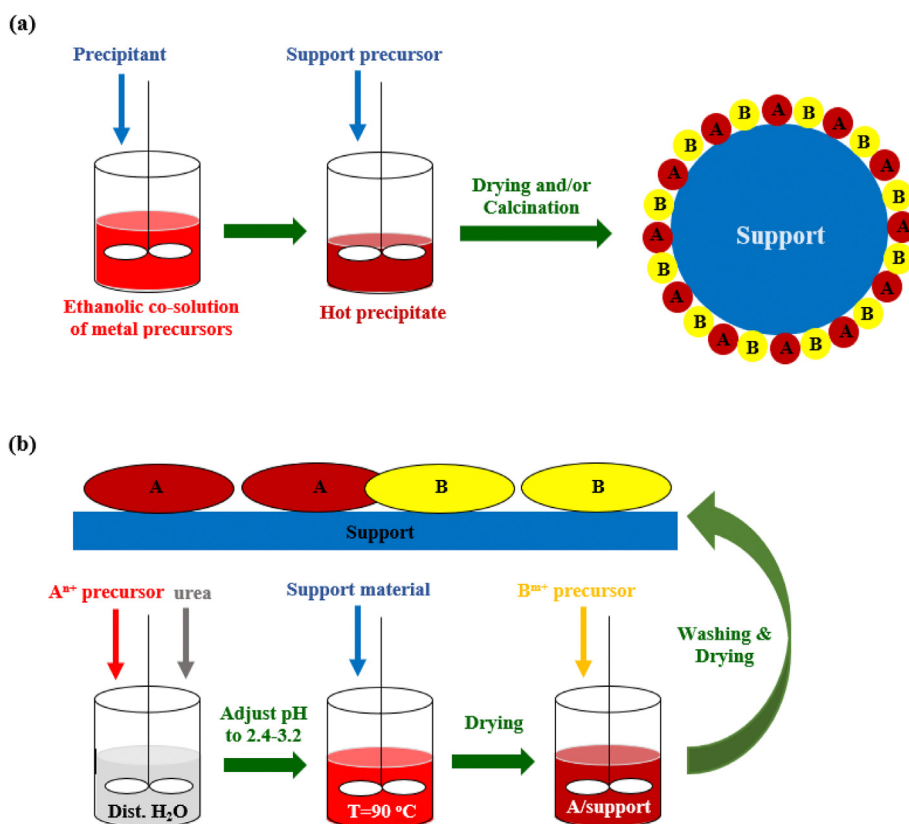


Fig. 2. Synthesis of supported bimetallic catalysts by (a) co-precipitation and (b) deposition precipitation.

3.2. Deposition precipitation

Deposition precipitation involves deposition from a precursor solution by changing the pH, temperature, or evaporation, resulting in metal compounds with relatively low solubility. Generally, an existing support is needed in this technique, and the concentration of the new compound is increased gradually to avoid the formation of bulk phases in solution (Van Der Lee et al., 2005). Preferential precipitation onto the support can be achieved by the introduction of the support into the solution, which causes either a surface free energy reduction of tiny nuclei or the stabilization of the precipitate, which consequently decreases the energy barrier for nucleation. The support surface must function as a seed for nucleation. The nucleation of a metal species is usually brought about by a change in pH, and thus compounds with a low solubility are produced. When this is done by injecting the precipitant, such as alkaline solution, utmost care must be employed to avoid local concentrations beyond the critical supersaturation, which would lead to bulk precipitation. Homogeneous deposition precipitation techniques are most often preferred, wherein precipitation is induced homogeneously throughout the reaction vessel. This can be done by the addition of urea, usually at room temperature, which when heated to 90 °C will slowly decompose, forming OH⁻. Consequently, slow enhancement of the pH upon decomposition occurs (Munnik et al., 2015). This method was developed for the synthesis of catalysts with metal loadings that exceed those produced by impregnation, which is limited by solubility (Van Der Lee et al., 2005).

In Fig. 2(b), the deposition precipitation technique is shown. The first metal precursor and urea are dissolved in distilled water with constant stirring, and then the initial pH of the solution is adjusted between 2.4 and 3.2 depending on the metal used. Subsequently, the support material is added to this solution. Thereafter, the suspension temperature is increased to 90 °C and kept constant for 16 h under continuous stirring. Urea decomposition usually leads to gradual rise in the solution pH above neutral pH. After being dried at 80 °C for a specified duration, the second metal is also deposited by deposition precipitation with urea. Then, these samples are washed, dried and stored for catalysis application (Munnik et al., 2015; Sandoval et al., 2013, 2011).

3.3. Plasma spraying

Plasma use in catalysis has been extensively studied (Kim et al., 2016; Mok and Kim, 2011; Neyts, 2016; Puliyalil et al., 2018; Wei et al., 2013). A few unusual chemical activities occur when plasma species are involved in catalyst surface reactions. This has led to efforts to apply plasma directly in the preparation of effective and efficient catalysts. There are three main trends in catalyst synthesis using plasma, namely the (1) plasma chemical synthesis of ultrafine particle catalysts, (2) plasma-assisted deposition of catalytically active compounds (on various carriers, particularly plasma spraying for the synthesis of supported catalysts using thermal plasmas), and (3) plasma-enhanced synthesis (or plasma modification of catalysts) (Liu et al., 2002).

Plasma comprises highly excited atomic, molecular, ionic, and radical species. It is considered to be the fourth state of matter. The plasma state is brought about by the ionization process that occurs when an ample amount of energy is applied to a gas. When the ingoing molecules collide with electrons and the absorption of electromagnetic radiation occurs, gas ionization takes place. The reactivity of the produced species depends on the type of plasma source and the gas utilized (Kizling and Järås, 1996). Generally, plasma is described to be an ionized gas that can be generated by electric discharges, plasma jet, radio frequency, etc. Plasmas are

classified as high- and low-temperature plasmas according to their energy level, temperature, and ionic density. High-temperature plasmas are usually used for nuclear applications. Low-temperature plasmas can be classified as thermal and cold plasmas. Thermal plasmas are generally used in the preparation of supported catalysts, particularly in the plasma spraying technique (Liu et al., 2002). The choice of plasma technique for a specific application is dictated by the target result.

The application of plasma techniques, including spraying and glow discharge plasma, for the synthesis of catalysts was first done in the 1980s. Plasma has currently attracted a lot of attention due to its potential in industrial applications in materials processing, including the development of commercial catalysts.

Metal substrates as catalyst supports pose advantages in catalytic application which make them more attractive than ceramic supports. Some of the main advantages include high mechanical strength and heat conductivity properties. The catalytic coatings should be protected from mechanical shock and chemical exposure to the reaction medium. In addition, the catalytic activity should be conserved at high temperatures. Plasma spraying offers the possibility of preparing solid surface coatings on metals exhibiting high mechanical and thermal stabilities. The application of this technology leads to possible synthesis of inert washcoats and catalytically active coatings (Ismagilov et al., 1999).

The principal scheme of powder plasma spraying configuration is presented in Fig. 3. In this study, alumina powders were sprayed to form a washcoating layer on titanium plates and nickel foam materials. Subsequently, the plasma sprayed layer was impregnated with lanthanum and cobalt cations to form the active phase leading to the synthesis of bimetallic La–Co catalyst (Ismagilov et al., 1999).

3.4. Impregnation

Impregnation is a process wherein a certain volume of solution containing the precursor of the active phase is contacted with the solid, either support or another active solid phase, which is then dried to remove the absorbed solvent. This is usually followed by the drying, calcination, and/or reduction of the impregnated support. One of the advantages of this method is its simplicity in practical operation at both the laboratory and industrial scales (Deraz, 2018).

3.4.1. Types of impregnation

Dry impregnation, generally called incipient wetness impregnation, capillary impregnation, or pore volume impregnation, infuses the desired support material with a solution that contains a precursor of the desired metallic species (Yu et al., 2012). In this

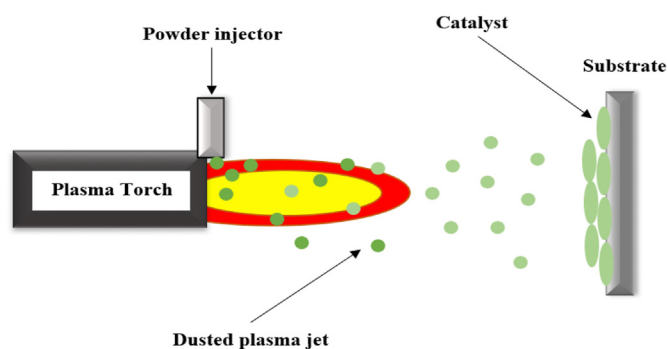


Fig. 3. Schematic diagram of the electrode configuration of. Discharge phenomena for plasma spraying.

type of impregnation, the support is impregnated with a volume of the precursor solution that is equal or slightly greater than the pore volume of the support material. Once the catalyst is impregnated into the support, it is then dried and calcined. The impregnated material maintains is dry at a macroscopic scale. According to the Young-Laplace equation, shown below, the uptake of the liquid into the pores of the support is caused by the capillary pressure difference Δp across a hemispherical meniscus in a pore with radius r_p .

$$\Delta p = \left(\frac{2\gamma_{lv}}{r_p} \right) \cos \theta \quad (2)$$

where γ_{lv} is the surface tension between the liquid and vapor interface and θ is the wetting angle between the solid and the liquid. When $\theta < 90^\circ$, the liquid is recognized to be wetting and penetrates the support spontaneously. The liquid is non-wetting when $\theta > 90^\circ$, whereby the capillary pressure becomes negative and external pressure is required to charge the liquid onto the pores (Munnik et al., 2015).

Wet impregnation, or soaking impregnation, involves the utilization of an excess solution with respect to the pore volume of the catalyst support. The solid catalyst is left to age after a certain length of time under stirring and is then filtered. The excess solvent is removed through drying. This technique is most commonly used when the precursor-support interaction can be anticipated. The metal precursor concentration depends on the concentration of the solution, support pore volume, and both the type and concentration of adsorbing active sites at the surface (Pinna, 1998).

3.4.2. Impregnation methods

Generally, impregnation is regarded as low-cost and easy to scale up, but unsuitable for bimetallic catalyst synthesis. The disadvantage of co-impregnation and sequential impregnation is that both methods form bimetallic particles with variable compositions. Co-impregnation (CIP) is simultaneous impregnation, wherein both metal precursor components in a single solution are impregnated into the catalyst support as shown in Fig. 4(a). Co-Fe/CeO₂ was synthesized with 10 wt% Co and 10 wt% Fe using CIP with an aqueous solution of cobalt and ferric nitrates (Rida et al., 2014). Subsequently, the solution was constantly stirred for 15 h at room temperature. Afterwards, the samples were dried and calcined. The synthesized catalyst was examined for its behavior toward CO oxidation. In sequential or successive impregnation (SIP), one metal is impregnated first, and then the impregnated catalyst is dried and

calcined to render it insoluble for the second impregnation step. After the calcination process, the second metal is impregnated to complete the synthesis of the bimetallic catalyst illustrated in Fig. 4(b) (Louis, 2016).

3.5. Sol-gel method

The sol-gel method is a promising technique for synthesizing catalyst supports due to its capacity to produce supports with a high surface area and high porosity. These properties facilitate the high dispersion of metal particles during the later impregnation step. This method also permits supported bimetallic catalyst synthesis in one step, leading to the dispersion of metal precursors during the catalyst support synthesis (Tran et al., 2007). Water can be used without a co-solvent as a reaction medium in the preparation stages, which makes the sol-gel method environmentally friendly (Sierra-Salazar et al., 2019).

Generally, the sol-gel method involves the polymerization of monomeric alkoxide precursors; for instance, tetraethyl orthosilicate (TEOS) is used in Fig. 5.

3.6. Reverse micelle method

Reverse micelle synthesis uses microemulsions to produce supported metallic particles with a relatively narrow size distribution. These microemulsions are formed by dissolving a small amount of metal precursors in an aqueous environment inside a nonionic surfactant such as Triton X-100 or cyclohexane. In Fig. 6, hydrazine (N₂H₄) is added as a reducing agent. The metal precursors are chemically reduced, which leads to the improvement of the Co-Fe particle formation in the core of the micelles (Mohd Zabidi et al., 2012). Synthesis of the supported catalyst starts when an aqueous solution is mixed with the metal precursors and a surfactant with an oil-phase solution of the reducing agent. Under vigorous stirring, the solution becomes clear, which indicates reverse micelle formation (Yu et al., 2012). The catalyst support is added as the solution is titrated with an emulsion destabilizing agent such as acetone or tetrahydrofuran (THF) to disrupt the micelles, which leads to the adsorption of the micelles onto the support (Mohd Zabidi et al., 2012; Yu et al., 2012).

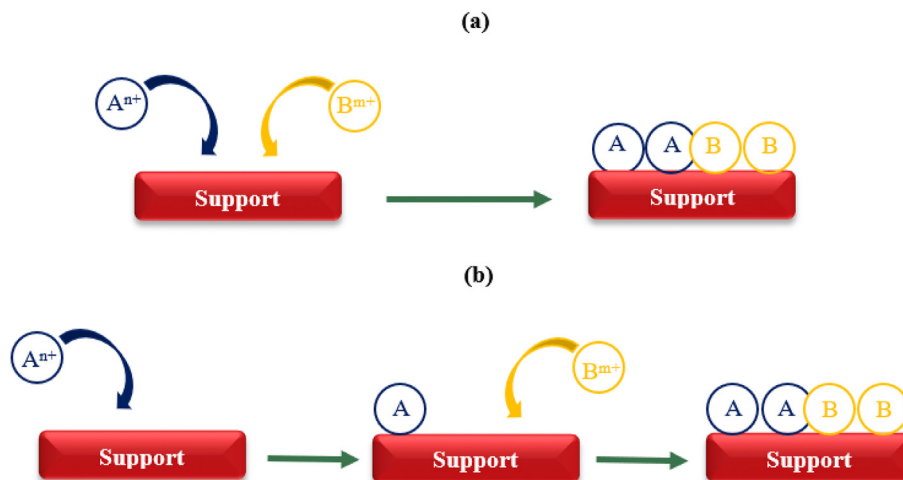


Fig. 4. Methods of impregnation as (a) co-impregnation and (b) successive impregnation.

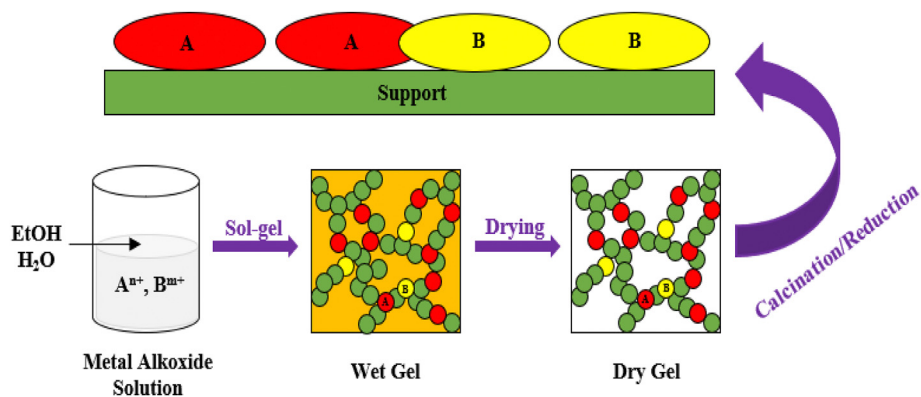


Fig. 5. Sol-gel synthesis of bimetallic supported catalyst.

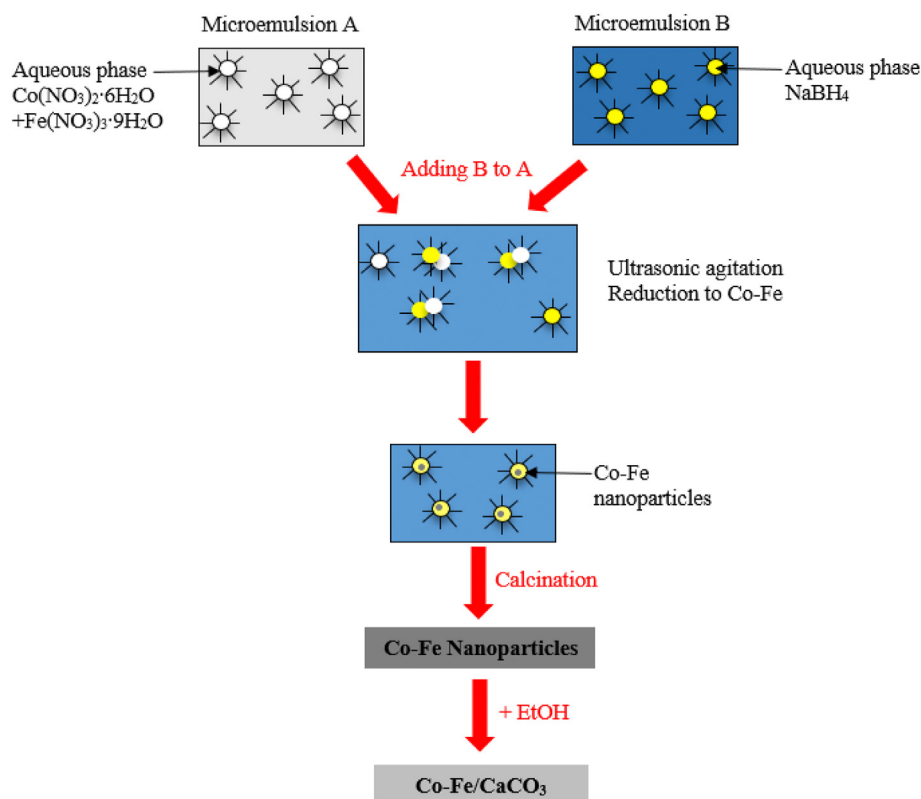


Fig. 6. Reverse micelle synthesis of bimetallic Co-Fe supported catalyst.

4. Catalytic application for contaminant remediation

Industrial wastewater may contain various recalcitrant organic compounds with variable toxicity and carcinogenic and mutagenic properties, which may lead to the pollution of the receiving water bodies. These organic compounds are generally persistent in the environment and may have adverse effects on human health and the ecosystem. Inorganic pollution of drinking water and its sources is caused by natural and anthropogenic factors. Management of these inorganic pollutants in water and wastewater is of prime importance due to their negative impacts.

4.1. Treatment of organic pollutants

Dye effluents cause serious environmental pollution worldwide.

There is thus growing interest in dye removal from water reservoirs for health and aesthetic reasons. Wastewater generated by the textile industry is known to contain appreciable amounts of non-fixed dyes, especially azo dyes, and a huge amount of inorganic salts (Riaz et al., 2012; Wu and Wen, 2010).

Aromatic compounds (involving phenol, chlorophenol, nitrophenol, and their derivatives) are very prevalent toxic pollutants. They have become great concerns due to their resistance to biodegradation and toxicity to humans and animals even at very low concentrations (Jiang et al., 2017). Phenols and their derivatives are chief organic constituents found in the waste discharges of coal tar, gasoline, plastic, rubber proofing, disinfectant, oil refining, petrochemical, pesticide, pharmaceutical, and steel industries, domestic wastewaters, agricultural run-off, and chemical spills (Jiang et al., 2017; Rani and Shanker, 2018). Phenols start to create a

characteristic odor at a very low concentration of about 5 mg L⁻¹ and pose a threat to aquatic life at 9–25 mg L⁻¹ (Villegas et al., 2016). According to the WHO, the drinking water standard is 1 mg L⁻¹ phenol (Jadhav and Vanjara, 2004). Phenols are thus major environmental pollutants in the range of 1–100 mg L⁻¹ due to their toxicity and recalcitrance and bioaccumulation properties. In this regard, phenols are categorized into specific priority pollutants (Rani and Shanker, 2018). Because of the toxicity of phenols and their derivatives in the environment, their effective and efficient removal from water and wastewater using low-energy-based techniques is mandatory.

Chlorinated organic compounds (COCs) are applied on a large scale in the chemical, petrochemical, and electronic industries. The environmental and health impacts of these contaminants have been extensively studied (Wang et al., 2009). Various chlorinated compounds, including CH₂Cl₂, CHCl₃, and CHClF₂, cause ozone depletion, and other COCs have negative effects on the human central nervous system and have been linked to diseases such as cancer (Xu et al., 2005b). Almost all chlorinated aromatic compounds have high toxicity and form a class of environmentally undesirable compounds that are associated with a broad range of industrial processes. Once released into the environment, they accumulate in the surroundings and endanger humans as well as the environment over a long period of time (Xu et al., 2005a).

4.1.1. Conventional treatment technologies

Various treatment technologies have been employed to remove dyes, including biological, thermal, physical, and chemical treatment methods. Some of these methods are not compatible with large-scale treatment. Biological treatment is unsuitable for treating non-biodegradable wastewater (as in the case of several dyes), and needs a relatively long retention time for the microorganisms to degrade the contaminants (Duarte et al., 2009; Ezzatahmedi et al., 2018; Ghuge and Saroha, 2018; Lee et al., 2004).

Conventional technologies such as adsorption, coagulation, and enzyme oxidation result in partial degradation to secondary pollutants. Biodegradation, physical separation, and advanced oxidation processes (AOPs) have received a lot of attention in recent studies for treating phenol- and phenolic-derivative-containing wastewater (Li et al., 2016). Physical separation using steam distillation, extraction, and membrane pervaporation has been widely studied. It was found to effectively remove phenol from wastewater and allow the recycling of phenol. These methods, however, have several disadvantages, including high energy demand for steam distillation, low efficiency for extraction, and high technical requirements for biodegradation (Jiang et al., 2017; Liotta et al., 2009).

In addition, COCs can also be eliminated by physical, biological, and chemical treatments. Physical treatment (e.g., gas blowing desorption, activated carbon (AC) adsorption, volatilization, and extraction) merely separates COCs from water and wastewater in terms of their physical properties (i.e., volatility and solubility) (Dvorak et al., 1993; Tütem et al., 1998). Additional cost is needed to treat the transferred COCs. Biological treatment can be applied for the decomposition of COCs by means of a metabolic process by microorganisms. However, it is inhibited by the toxicity of COCs toward microorganisms, the selectivity of microorganisms to specific contaminants, and the slow degradation rate of COCs (Broholm et al., 1993; Phelps et al., 1991; Strandberg et al., 1989; Trapido et al., 1998). Chemical treatment includes the Fenton process, incineration, ozone oxidation, photocatalytic oxidation, and wet oxidation (Kim et al., 2007). Oxidation processes degrade COCs into CO₂, H₂O, and HCl (Wang et al., 2008).

4.1.2. Dye degradation

To overcome the drawbacks of conventional methods, bimetallic catalysts have been extensively studied for the remediation of dye-containing effluents. Different bimetallic catalysts have been applied to treat dye-containing wastewater. Fe–Ni bimetallic nanoparticles (BNPs) were synthesized to completely degrade Orange G (OG) with an initial concentration of 150 mg L⁻¹ (pH: 3, catalyst dosage: 3 g L⁻¹, T = 28 ± 2 °C, reaction time: 10 min) (Bokare et al., 2007). SBA-15 supported Fe–Ni was investigated leading to 99.3% degradation of Acid Red 73 (AR73) by Fenton-like reaction. Using monometallic catalysts, Fe/SBA-15 and Ni/SBA-15, showed poor AR73 removal efficiency achieving 29.2% and 21.9% degradation, respectively. It is obvious that the bimetallic catalyst achieved high catalytic activity implying that synergistic effect between Fe and Ni exists for AR73 removal (Li et al., 2015).

Cu–Ni/TiO₂ was synthesized via deposition precipitation and wet impregnation to treat dye at a concentration of 50 mg L⁻¹ using visible light via photocatalysis (Riaz et al., 2014). It was found that bimetallic catalyst can efficiently and completely degrade dyes, in this case, Orange II (OII). When treating the same contaminant with Cu–Ni/TiO₂ synthesized by co-precipitation, complete degradation was achieved within 60 min at room temperature (Riaz et al., 2012). Similarly, complete degradation was observed at the end of 90 min for Rhodamine 6G treatment using Cu–Fe supported on ZSM-15 zeolite. It was also found that the catalytic performance of this bimetallic catalyst is far better than that of the monometallic Fe/ZSM-15 catalyst (Dükkanci et al., 2010).

Complete photodegradation of Acid Violet 7 (AV7) was reached with an initial concentration of 300 mg L⁻¹ using UV light for 60 min using Cd–Ag/ZnO. 72% removal was achieved using Cd/ZnO while 82% degradation was reached with Ag/ZnO. Acid Black 1 (AB1) was also targeted achieving 98% degradation within 45 min using the same bimetallic catalyst. Using Cd/ZnO and Ag/ZnO catalysts led to 84% and 82% AB1 removal, respectively. Results show enhancement in both AV7 and AB1 degradation efficiency using the bimetallic catalyst (Balachandran and Swaminathan, 2012). In addition, complete degradation of Reactive Orange 4 was reported using catalytic ozonation for 100 mg L⁻¹ initial dye concentration at pH 9 (Ghuge and Saroha, 2018). In this work, catalytic ozonation was also performed to treat an actual textile dye industry effluent using Ru–Cu/SBA-15 bimetallic catalyst containing a high concentration of bicarbonate ions and chemical oxygen demand (COD) of about 1360 and 1440 mg L⁻¹, respectively. It was shown that the presence of bicarbonate ions in the textile industry dye effluent caused low COD removal efficiency (30.88%) in the system. These bicarbonate ions are said to act as hydroxyl radical scavengers (Zhao et al., 2011). Thus, they should be removed from the effluent prior to its catalytic treatment.

OII was also completely degraded using diatomite-supported Fe–Ni NPs at pH 3 (Ezzatahmedi et al., 2018). The use of Fe–Ni supported on SiO₂ as a heterogeneous photo-Fenton catalyst under solar and visible light irradiation to treat methylene blue (MB) was reported (Ahmed et al., 2016). In this study, both degradation and total organic carbon (TOC) removal efficiencies were higher using solar light than using visible light. The bimetallic catalyst presented good catalytic activity and was observed to respond to hydrogen peroxide to produce hydroxyl (•OH) radicals in the degradation of MB dye molecules. A mechanism for the degradation of dyes is shown in Fig. 7 (Pradhan et al., 2016). In the photo-Fenton system, dye degradation progresses in the presence of Co–Fe/Al₂O₃–MCM-41 catalyst, hydrogen peroxide (H₂O₂), and visible light. The oxidation and reduction reactions occur from Co²⁺–Fe²⁺/Al₂O₃–MCM-41 to Co³⁺–Fe³⁺/Al₂O₃–MCM-41 nanocomposite, stimulating •OH radical generation. The •OH radicals react with dye molecules and produce a degradation product. In the

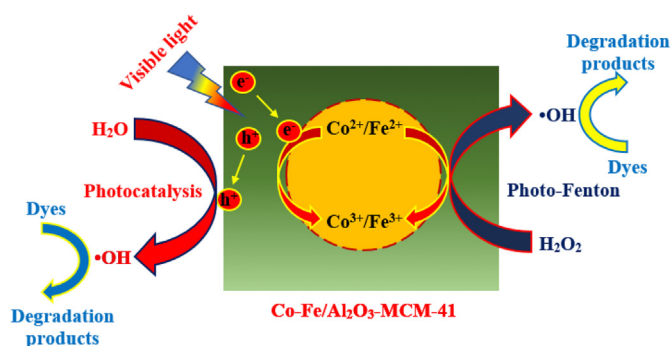


Fig. 7. Mechanistic pathways of dye degradation using Co-Fe/Al₂O₃-MCM-41 in visible light.

case of photocatalysis, electrons (e^-) and holes (h^+) are generated when the surface of the bimetallic catalyst is exposed to visible light. h^+ reacts with H₂O and then forms the active species (\bullet OH radicals). The photogenerated electron reacts with dissolved O₂. Consequently, the generated \bullet OH radicals react with dyes, producing degradation products (Pradhan et al., 2016).

Different bimetallic catalysts supported on alumina-mesoporous silica were studied in the photodegradation of MB, Congo red (CR), and mixed dyes (MB + CR). The photodegradation order for all the dyes treated is Co-Fe/Al₂O₃-MCM-41 > Fe-Mn/Al₂O₃-MCM-41 > Mn-Co/Al₂O₃-MCM-41 > Fe/Al₂O₃-MCM-41 > Co/Al₂O₃-MCM-41 > Mn/Al₂O₃-MCM-41. The results indicate that adding a second metal improves the catalytic activity and performance of the monometallic catalyst (Pradhan et al., 2016). CR was also treated using hydrogen peroxide and Co-Fe supported on polyacrylamide hydrogel (PAM) as the oxidant and catalyst (with a loading of 0.05 g L⁻¹), respectively, at neutral pH, reaching about 96.45% efficiency within 60 min. In addition, Fe/PAM and Co/PAM were used to determine the effect of second metal incorporation in the CR removal leading to 85.19% and 84.76% degradation within 75 min, respectively (Aftab et al., 2019). Cobalt and iron supported on mesoporous SBA-15 was utilized in OII degradation, achieving 93.4% at room temperature under acidic conditions (Cai et al., 2015). Co-Fe catalysts achieved different degradation efficiencies depending on the support used, the synthesis method utilized, and the target dye pollutant treated (Aftab et al., 2019; Cai et al., 2015; Pradhan et al., 2016).

Recently, Cu-Ni supported on ginger powder (GP) has been used to treat three kinds of dye (Ismail et al., 2018). The 3.0 g L⁻¹ Cu-Ni (combined with sodium borohydride electrolyte) showed good catalytic activity for the removal of various dyes, i.e., Rhodamine B (RhB), Methyl Orange (MO), and CR, with 95–98% removal. Moreover, the Cu-Ni catalyst was compared with the Cu-Ag catalyst, showing similar degradation efficiencies for all the dyes studied at a very short reaction time. The reusability of Cu-Ni/GP and Cu-Ag/GP catalysts was found to be five cycles. The use of Cu-Ag/GP catalysts can completely degrade the dyes after a series of five cycles for 4, 5, 7, 10, and 12 min for each respective cycle. The use of Cu-Ni/GP leads to longer reaction times to accomplish complete degradation in its series of five cycles (i.e., 5, 7, 9, 14, and 19 min). Consequently, the stability of the synthesized GP-supported catalysts was checked after 1, 18, and 36 h. Both catalysts (Cu-Ag and Cu-Ni) were stable, demonstrating almost complete degradation of MO dye (with 90% efficiency). However, Cu-Ag can degrade the dye in a shorter time (approximately half the time relative to Cu-Ni).

The recyclability results indicated that Cu-Ag/GP has excellent reusability and stability compared with those of Cu-Ni/GP.

Therefore, Cu-Ag/GP catalyst can be utilized many times as an active catalyst in various chemical reactions. The exceptional catalytic activity of Cu-Ag/GP during reuse compared to that of Cu-Ni/GP might be due to the excellent absorption capability of GP for copper and silver and due to the higher reduction potential of silver compared to that of nickel. Furthermore, the Cu-Ni/GP catalyst may be oxidized during the reduction process (Ismail et al., 2018).

Mesoporous SBA-15 supporting iron and nickel was utilized to degrade 99.3% of 50 mg L⁻¹ AR73. The optimal Ni-to-Fe ratio was 1:2. In this study, the catalyst showed high catalytic activity with 95% efficiency even after seven consecutive cycles (Li et al., 2015). Similarly, this high catalytic activity was exhibited for the removal of Direct Black G (DBG) (Liu et al., 2013). The reusability of this catalyst was tested in treating actual wastewater from a textile printing and dyeing company in Fuzhou, China. The degradation rates were 99.01%, 94.57%, and 49.21% after the first, third, and fifth cycles, respectively, demonstrating a drastic decrease in degradation rate with the number of cycles. Moreover, it was shown that kaolin serves as an adsorbent for DBG and as a stabilizer for Fe-Ni NPs. DBG was degraded by the synthesized catalyst via the adsorption of kaolin and a redox reaction of Fe-Ni, with Ni acting as a catalyst and Fe acting as a reductant. Furthermore, the Fe-Ni catalyst was shown to be highly effective for treating MB via the solar and visible photo-Fenton process (Ahmed et al., 2016).

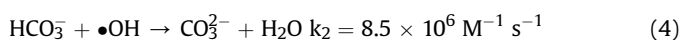
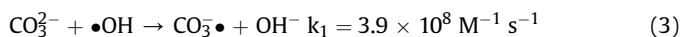
The performance and catalytic activity of Cu-Ni catalyst supported on titania synthesized by co-precipitation, deposition precipitation, and wet impregnation were compared accordingly (Riaz et al., 2012). The catalyst prepared by wet impregnation gave the highest degradation efficiency under the same operating conditions; this was confirmed by another study (Hameed, 2016). The authors used Cu-Ni/TiO₂ and Cu-Ni/ZnO, achieving 97.74% and 76% Vat Red 1 dye degradation, respectively. Similarly, Fe-Cu/ZSM-5 was synthesized using the ion-exchange (IE) and hydrothermal (HT) methods. HT-Fe-Cu/ZSM-5 removed 99% of Rhodamine 6G (100 mg L⁻¹) at pH 3.5 after 120 min. IE-Fe-Cu/ZSM-5 achieved complete degradation at a higher pH (pH 7.2) after 90 min of reaction (Dükkanci et al., 2010).

Fe-Cu/HMS, Fe/HMS and Cu/HMS systems via heterogeneous Fenton catalysis were compared in terms of OII abatement. Fe/HMS and Cu/HMS as the catalysts reached 31.6% and 85.7% OII reduction for 2 h of reaction, respectively, reflecting relative inert catalytic activity of Fe/HMS compared to that of Cu/HMS. Significantly, Fe-Cu/HMS achieved 94.3% degradation in 2 h, which clearly shows the synergistic effect of iron and copper in the Fenton reaction (Wang et al., 2015). It was found that the addition of Cu on the Fe catalyst produced a catalyst that is less pH-dependent while maintaining high activity. At pH 9.0, it still showed a high catalytic degradation of 93.8%. This catalyst retained high catalytic activity after five consecutive runs (78.9%) (Wang et al., 2015). Fe-Cu catalyst was observed to exhibit good performance in treating OII dye, reducing the concentration from 100 to 7.2 mg L⁻¹ (92.8%) with Fe-Cu/HMS catalyst (Wang et al., 2016). Fe/HMS and Cu/HMS achieved 23.8% and 85% removal, respectively, indicating the superiority of the bimetallic catalyst in terms of performance and activity. Furthermore, this catalyst was applied to treat a high initial concentration (1000 mg L⁻¹ OII), with 77.71% removal efficiency at pH 7.0. The fabricated Fe-Cu/HMS had good stability and recyclability performance (about 75.1% after 5 runs). The optimal Fe/Cu ratio was 1:3 (Wang et al., 2016). It was found that the catalytic activity of the bimetallic catalyst highly depends upon the Fe/Cu ratio. Similarly, 94.3% OII removal was achieved at pH 7.0 using Fe-Cu catalyst supported on carbon nanofibers (CNF) (Wang et al., 2017). Obtained OII removal efficiencies using Fe/CNF and Cu/CNF are 18.5% and 69.3%, respectively. The prime catalytic activity of

Fe–Cu/CNF can be attributed to the synergistic effect between iron and copper enhancing the performance and activity of this catalyst in Fenton catalysis. After 5 cycles, 79.9% OII degradation was achieved, exhibiting good recyclability performance in the heterogeneous Fenton process (Wang et al., 2017). For these progressive works, the support might have a significant effect on the degradation efficiency despite treating the same dye contaminant (Wang et al., 2017, 2016, 2015).

Fe–Cu bimetallic catalysts supported on bentonite and amoxidized polyacrylonitrile fiber complexes also showed high catalytic performance for treating AB1 and RhB dyes, respectively (Dong et al., 2011; Yip et al., 2007). Fe–Cu supported on acid-activated bentonite reached 99%–100% degradation at all pH values (pH 3 to 9), indicating high catalytic activity. In addition, TOC removal efficiencies were found to be 90%, 85%, and 94% for pH 3, 7, and 9, respectively (Yip et al., 2007).

The Fe–Mn catalyst can also be used to treat MB and CR dyes. Specifically, Fe–Mn/Al₂O₃–MCM-41 exhibited 97% and 90% MB and CR dye degradation, respectively (Pradhan et al., 2016). Wet impregnation-synthesized Fe–Mn supported on granular activated carbon (GAC) reduced 50 mg L⁻¹ MO dye by 94% via catalytic ozonation (Tang et al., 2016). In this work, the catalyst (5 g L⁻¹ at ambient temperature with pH 10.0) exhibited good catalytic activity. Furthermore, the influence of •OH radical scavengers on MO removal was examined. The study adopted sodium carbonate as the free radical scavenger added into the MO simulated wastewater. It was observed that the MO removal decreased with increasing Na₂CO₃ dose. Remarkably, 99% MO removal was achieved with Na₂CO₃ added in the wastewater. Approximately 85%, 71%, and 65% of MO could be degraded at Na₂CO₃ dosages of 5, 10, and 20 mL, respectively, under the same conditions. As stated above, the main reason is that carbonate (CO₃²⁻) and bicarbonate ions (HCO₃⁻) are generally considered as •OH scavengers; both can react with •OH to generate carbonate radical ions through the following reactions in an appropriate pH range (Hao et al., 2012):



where k is the rate constant of CO₃²⁻ and HCO₃⁻, correspondingly.

This shows that the addition of •OH scavengers decreases MO degradation and proves that the main mechanism for MO degradation is the generation of •OH by the catalytic ozonation of the Fe–Mn catalyst supported on GAC.

Unsupported bimetallic NPs were also used as heterogeneous catalysts for the treatment of dye-containing effluents. Fe–Ni NPs were found to be effective catalysts for OG dye degradation. Bokare et al. observed complete degradation with an initial concentration of 1500 mg L⁻¹ at pH 7 (Bokare et al., 2007). Similarly, in acidic conditions (pH 2.0), OG was 100% degraded after 10 min of reaction (Bokare et al., 2008). 98% removal was observed with a high initial concentration of 1000 mg L⁻¹ for 60 min of treatment (Foster et al., 2019). Similarly, Fe–Cu unsupported catalysts can be used to treat 1000 mg L⁻¹ Acid Orange 7 dye, reducing it by 94.3% with the aid of sodium sulfate (Yuan et al., 2014). The authors suggested that this bimetallic system is a promising process for the toxic and refractory wastewater from the printing and dyeing industries, significantly reducing the TOC and COD by 60.8% and 61.8%, respectively. An iron-palladium catalyst was found to have high stability even after 28 days, maintaining 75.1% degradation.

Recently, Fe–Ni metal organic frameworks (MOFs) were found to be efficient Fenton-like catalysts for the treatment of MB and MO dyes under visible light. These bimetallic catalysts possessed significantly enhanced adsorption and photo-Fenton performance

compared with monometallic catalysts, and simultaneous in situ decontamination and adsorbent regeneration (Wu et al., 2021). Activated carbon derived from waste lemon by-products was used as a support material for Fe–Zn bimetallic nanoparticles. The activity of the catalyst was studied on its catalytic action on Reactive Red 2 dye (100 mg L⁻¹) in the Fenton-like system leading to 96.01% degradation (Oruç et al., 2019). Monometal- and bimetal-doped MCM-41 (Fe/MCM-41, Co/MCM-41 and Fe–Co/MCM-41) were utilized to degrade synthetic MO dye wastewater via PMS activation. Compared with its monometallic counterparts, the bimetallic catalyst showed extremely higher catalytic activity and stability, and remarkably lower metal leaching in the catalytic oxidative degradation process. This excellent activity could be attributed to the high metal dispersion and the synergistic effects of Co²⁺/Co³⁺ and Fe²⁺/Fe³⁺ redox cycles (X. Sun et al., 2020). A porous biochar-supported Fe–Mn composite was found to be an effective persulfate activator for Acid Red 88 degradation together with its high stability and reusability (Chen et al., 2020). Pd–Ag supported on macroporous silicon (macroPSi) was fabricated for MB degradation. Photocatalytic activity of the monometallic and bimetallic catalysts was tested under ultraviolet irradiation. Pd–Ag/PSi exhibited higher activity than the as-prepared macroPSi, Ag/PSi and Pd/PSi showing superior performance (Wali et al., 2019). Bimetallic Au–Pd NPs were deposited on a hybrid of Na₂Mn₄O₁₃ and MoO₃ (NM) to synthesize highly active and stable nano-hybrid bimetallic catalysts. The performance of monometallic and bimetallic systems was compared in the treatment of Safranin, Brilliant Green and Methylene Blue dyes. The catalytic activity observed in this work is as follows: Au–Pd/NM > Au/NM > Pd/NM. It was also found that the highest catalytic activity for dye degradation is achieved using Au/Pd mass ratio of 1:1 and calcination temperature of 400 °C (P. Wang et al., 2020). Highly active Cu–BiOS bimetal oxysulfide catalysts were efficient in the reduction of organic dyes (MB, MO and RhB) in the presence of NaBH₄ under dark condition within 3 min of reaction time (Guo et al., 2020). MO catalytic reduction using bimetallic Au–Ag catalyst and NaBH₄ reductant reached complete degradation showing higher catalytic reduction activity than the monometallic Ag catalyst (55.25%) (Vinotha Alex et al., 2020). Photodegradation of RhB under visible light illumination was done using bimetallic Al–Fe MOF achieving almost complete degradation in 120 min. Improved photo-Fenton catalytic efficiency, recyclability, higher reliability and stability than its parent MIL-88 B(Fe) (MIL: Materials Institute Lavoisier) were achieved by this catalyst. In addition, no significant metal leaching was observed during the photodegradation process. These characteristics notably justify its economic feasibility in real applications (Nguyen et al., 2020). The Fenton catalytic performance of Cu–Co MOF embedded on carbon nanocubes (CNC) were investigated in the degradation of AOII. The Cu/Co ratio of 4:6 displayed the highest catalytic activity with faster degradation rate than Co/CNC. The catalytic performance of the bimetallic catalyst could be attributed to the synergistic effects of the optimized ratio of Cu/Co, high surface area and graphitized carbon framework. Furthermore, notable reusability performance was observed after five successive runs (90.6%) (J. Wang et al., 2020). Copper-based bimetallic oxysulfide (CuVOS) coated on the surface of spherical porous SiO₂ (CuVOS/SiO₂) was investigated for the catalytic reduction of MB, MO and RhB showing complete degradation for all the studied dyes in less than 5 min under similar conditions. It was also found that the porosity of the SiO₂ support and the active sites of CuVOS in the bimetallic system enhanced the catalytic reduction under dark conditions (H. Sun et al., 2020).

Dye degradation by bimetallic catalytic activity depends on the metal ratio, choice of support, degradation process, catalyst loading, temperature, pH, and initial dye degradation. Bimetallic

catalysts are promising for the remediation of dye-containing water and wastewater and can be used in a wide range of pH values. They have high reusability and stability, which are an advantage in heterogeneous catalysis.

4.1.3. Degradation of phenol and its derivatives

Peroxymonosulfate (PMS) activated by Cu–Co/MnO₂ is 100% efficient in the degradation of phenol in the heterogeneous decomposition system. Monometallic catalysts, Cu/MnO₂ and Co/MnO₂, were compared to the bimetallic catalyst achieving 47.3% and 61.6%, respectively, showing the significant effect of adding a second metal. A remarkable synergistic effect from Co and Cu in MnO₂ was evidenced in this study (Khan et al., 2017). Similarly, complete degradation of a high phenol concentration of 1000 mg L⁻¹ was achieved by Jiang et al. via catalytic wet peroxide oxidation (CWPO) catalyzed by Fe–Cu/ZSM-5 within 7 h (Jiang et al., 2017). Sun et al. treated the same initial concentration at a shorter period of 3 h (Sun et al., 2017). 500 mg L⁻¹ phenol was completely degraded using Au–Pd/TiO₂ catalyst under UV–visible irradiation, suggesting a high oxidative degradation capacity of bimetallic catalysts toward phenol. Au/TiO₂ and Pd/TiO₂ both reached below 60% phenol degradation efficiency showing lesser catalytic activity from Au–Pd/TiO₂ catalyst (Cybula et al., 2014). The possible contribution of iron to the HDC activity of bimetallic Pd–Fe/γ-Al₂O₃ catalyst for chlorophenols was investigated using monometallic Fe/γ-Al₂O₃ catalyst showing no significant HDC activity. CWPO was applied to the phenol formed from the hydrodechlorination (HDC) of 4-chlorophenol, achieving 100% degradation within 1 h (Munoz et al., 2013). Almost complete degradation was reached using Co–Ni supported on a N-doped carbon matrix (NC) for treating less than 500 mg L⁻¹ phenol, with ≥99.9% of it converted to cyclohexanol. Co/NC and Ni/NC both revealed poor catalytic activity achieving 35.2% and 23.2% cyclohexanol conversion (Li et al., 2017). Moreover, high degradation efficiency (98%) was observed using Fe–Cu/allophane clays achieving greater catalytic activity compared to that of Fe/allophane and Cu/allophane catalyst under identical conditions (Garrido-Ramírez et al., 2016). Various Fe-based bimetallic catalysts were tested for treating 1000 mg L⁻¹ phenol solution, achieving 100%, 97%, and 70% degradation for Fe–Mn, Fe–Co, and Fe–Ni catalysts, respectively, under the same operating conditions (Sun et al., 2017). The Fe–Mn catalyst was also tested for three runs; it retained 100% degradation, indicating its great catalytic reusability for phenol treatment. Similarly, NC-supported Cu–Ni, Cu–Co, and Co–Ni were tested for phenol degradation in the presence of H₂. It was found that the degree of degradation followed the order Co–Ni ≫ Cu–Co > Cu–Ni (Li et al., 2017).

Fe and Fe–Cu supported on hollow Silicate-1 (hol S-1) were also investigated for phenol degradation. The bimetallic catalyst showed superior catalytic activity (~100% degradation) compared to the monometallic catalyst (~70% degradation). The Fe and Cu leaching in the system are 0.28 and 0.35 mg L⁻¹, respectively, which is an advantage in the heterogeneous catalysis system. After 5 cycles, Fe–Cu/hol S-1 still degraded 80% of phenol while Fe/hol S-1 only reached 20% degradation indicating the enhancement of the catalytic activity upon addition of Cu to the monometallic catalyst (Dai et al., 2017). Similarly, Fe–Cu supported on aluminum-containing MCM-41 Fenton catalyst was synthesized via coprecipitation. 47% TOC reduction was achieved at pH 4, 0.049 M of H₂O₂ dosage and temperature of 60 °C. Compared with the monometallic catalysts, the synthesized bimetallic catalyst exhibited a higher activity and greater stability in phenol mineralization (Xia et al., 2011).

Phenol degradation by Co–Cu bimetallic catalyst is shown in Fig. 8 (Khan et al., 2017). When PMS is activated in the presence of

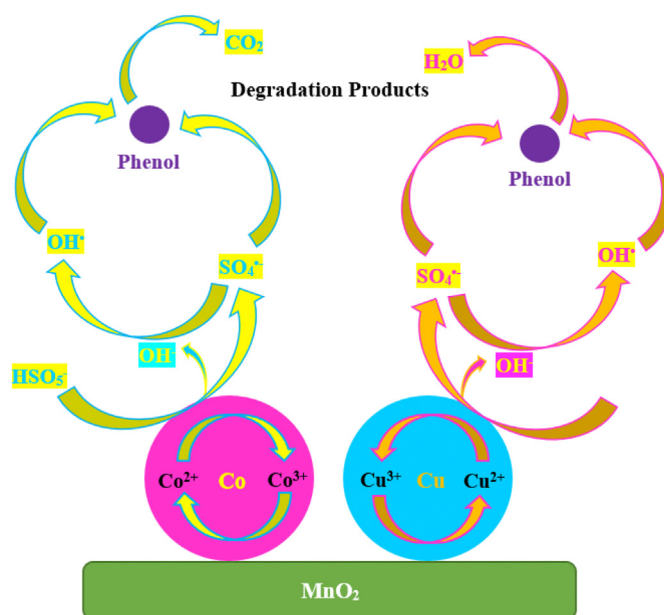
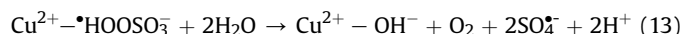
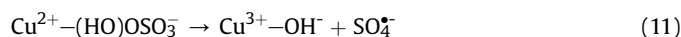
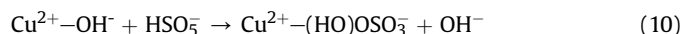
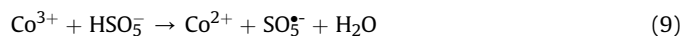
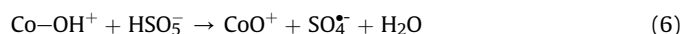


Fig. 8. Phenol degradation pathways by bimetallic catalyst.

Cu²⁺, the Cu²⁺–(HO)OSO₃⁻ complex forms through one electron transfer inside this complex. Consequently, SO₄^{•-} is produced and Cu³⁺–OH⁻ is generated, which is then reduced to Cu²⁺–OH by HSO₅⁻. Cu²⁺–(HO)OSO₃⁻ is formed by the interaction between the metal site and the peroxy-bond in PMS. This mechanism is described by the following reactions:



The photocatalytic activity of Au–Cu/TiO₂ have been studied for phenol photodegradation in aqueous solutions under UV–visible irradiation. Surprisingly, addition of Cu to Au/TiO₂ led to better enhancement in the photocatalytic properties of Au/TiO₂. Using the bimetallic catalyst, the phenol photodegradation reached 80% in 3 min and complete degradation in 6 min. The kinetic degradation is in the order: Au–Cu/TiO₂ > Cu/TiO₂ > Au/TiO₂ which indicates improved photocatalytic activity utilizing the bimetallic catalyst (Hai et al., 2013).

Bimetallic catalysts were also found to be viable catalysts for the treatment of chlorophenols with a concentration of as high as 200 mg L⁻¹. 200 mg L⁻¹ of 4-chlorophenol (4-CP) was treated,

reaching complete degradation with a Pd–Fe/ γ -Al₂O₃ catalyst dose of 2 g L⁻¹ and 10.15 mM H₂O₂ concentration within 1 h (Munoz et al., 2013). Similarly, Pd–Fe and Rh–Fe catalysts supported on γ -Al₂O₃ were observed to completely degrade the same concentration of 4-CP, achieving 84.9% phenol selectivity and 99.9% cyclohexanol selectivity, respectively (Munoz et al., 2014). 99.9% 4-CP degradation, 51.0% COD removal and 40.2% TOC removal were observed using the Cu–Co catalyst supported on alumina in an H₂O₂/HCO₃⁻ system. To determine the effect second metal incorporation, alumina-supported Co and Cu catalysts were also synthesized and used achieving poor 4-CP degradation, TOC and COD removal compared to the bimetallic catalyst (Li et al., 2016). Furthermore, the treatment of 20 mg L⁻¹ 4-CP was catalyzed by Fe–Ni supported on montmorillonite (MMT), reaching complete degradation (Zhang et al., 2019).

2,4-dichlorophenol (2,4-DCP) and 2,4,6-trichlorophenol (2,4,6-TCP) were treated using various bimetallic catalysts, with the Pd–Fe catalyst exhibiting superior catalytic degradation capacity. The Pd–Fe/ γ -Al₂O₃ catalyst exhibited total degradation with an initial 2,4,6-TCP concentration of 100 mg L⁻¹ in the H₂O₂ system (Munoz et al., 2013). Almost complete degradation (99.9%) of 50 mg L⁻¹ 2,4,6-TCP in the H₂O₂/HCO₃⁻ system was reported (Li et al., 2016). With the same Pd–Fe/ γ -Al₂O₃ catalyst, 200 mg L⁻¹ 2,4-DCP was treated, with complete removal achieved within 1 h (with a catalyst dose of 2 g L⁻¹ and 10.15 mM H₂O₂ concentration at room temperature) (Munoz et al., 2013). Moreover, the Pd–Fe catalysts were further utilized to treat 2,4-DCP with concentrations in the range of 10–200 mg L⁻¹, with 90%–100% degradation achieved (compared to Fe–Cu catalyst achieving 76.3% degradation with 10 mg L⁻¹ concentration) (Fang et al., 2018; Li et al., 2016; Wei et al., 2006; Witońska et al., 2014; Zhang et al., 2010). For parachlorophenol treatment, Pd–Fe was found to be an efficient bimetallic catalyst for treating a concentration range of 5–100 mg L⁻¹ (Jovanovic et al., 2005; Su et al., 2011; Zhou et al., 2013). In addition, 500 mg L⁻¹ para-nitrophenol was 98% degraded with a catalyst dose of 35 g L⁻¹ in the presence of sodium sulfate at pH 6.7 (Lai et al., 2014).

20 mg L⁻¹ of 4-NP took only 2 min to be completely degraded by CuVOS/SiO₂ bimetallic catalyst under dark condition (H. Sun et al., 2020). Similarly, bimetallic CuBiOS oxysulfide catalyst was used for the complete reduction of 4-NP in the presence of NaBH₄ within 2 min (Guo et al., 2020). Mesoporous silica modified with graphitic carbon nitride was used as support for Au–Pd bimetallic NPs. This synthesized photocatalyst showed superior photocatalytic activity compared to the monometallic catalyst in the mixed Cr(VI)/phenol solution ascribing to its enhanced visible light response and bimetallic co-effect. In this study, simultaneous reduction of Cr(VI) and oxidation of phenol occurred (Patnaik et al., 2020). Fe–Ni nanocomposite supported on sepiolite (Fe–Ni/Sep) was used to degrade 2,4-DCP from aqueous solution. The pollutant was completely degraded using the bimetallic catalyst, whereas Fe–Ni nanocomposite and sepiolite in isolation yielded 90.8% and 8.4% removal efficiencies, respectively. TOC removal efficiencies were 92.9%, 84.7% and 9.2% for Fe–Ni/Sep, Fe–Ni nanocomposite and sepiolite, respectively, indicating higher catalytic performance using the bimetallic catalyst (Ezzatahmedi et al., 2019a). In another work, Fe–Ni bimetallic catalyst supported on palygorskite (Fe–Ni/Pal) was used as a heterogeneous catalyst for 2,4-DCP dechlorination. Complete dechlorination and 2,4-DCP degradation was observed together with high TOC removal efficiency. Fe–Ni/Pal showed higher dechlorination performance and TOC removal efficiency than Fe–Ni composite and Fe/Pal catalysts (Ezzatahmedi et al., 2019b). Fe–Cu/zeolite Fenton-like catalyst was found to be more efficient on phenol degradation at near neutral pH than Fe/zeolite and Cu/zeolite. In the presence of H₂O₂, the supported

bimetallic catalyst was able to remove 95.3% phenol after 4 h of reaction time at pH 5, which was much higher than that of the monometallic catalysts under identical conditions. The improved catalytic activity of Fe–Cu/zeolite was brought about by the synergistic effect between the Fe/zeolite (core) and the two-dimensional copper hydroxide nanosheets (shell). The Cu hydroxide nanosheets with an open network structure on Fe–Cu/zeolite surface enhanced the stability of the Fe(III) under acidic conditions and avoided reduced catalytic efficiency of Fe(III) cause by embedding effect (Huang et al., 2020).

Fe–Cu/zeolite was also utilized to treat bisphenol A (BPA) achieving 87% degradation with catalyst dose of 3 g L⁻¹, Cu/Fe ratio of 1:2 and pH 5 within 120 min. The bimetallic catalyst used possessed advantages such as easy preparation, relatively low chemical cost, high production of reactive oxygen species and easy operation for upscale applications (Xu et al., 2020). Co–Bi bimetallic NPs were functionalized with nickel foam (NF) and were employed as heterogeneous catalysts in the activation of PMS targeting BPA as pollutant achieving 95.6% removal within 30 min. Co/NF and Bi/NF were also investigated, and the results show that Bi/NF was not capable in activating PMS with no BPA degradation occurring while Co/NF–PMS system achieved 39.9% BPA degradation after 30 min. The synergistic effect of cobalt and bismuth played a significant role in the heterogeneous catalysts as PMS activators. Co–Bi/NF showed superior catalytic activity on BPA degradation, especially when the calcination temperature and time were 300 °C and 2 h, respectively. In addition, this bimetallic catalyst also exhibited outstanding reusability and stability (Hu et al., 2019). Similarly, Fe–Co bimetallic catalyst with Fe/Co ratio of 1:1.12 was utilized to treat BPA pollutant reaching 96% removal in 2 min. Significantly, the stability test showed that the rich Fe on the shell section could effectively inhibit cobalt ion leaching (Zhang et al., 2020).

Fe–Co catalyst as PMS activator treated 20 mg L⁻¹ phenol solution achieving complete degradation in 30 min at room temperature. Different calcination temperatures were also investigated showing that the bimetallic catalyst calcined at 300 °C exhibited excellent catalytic stability owing to the minimal to negligible Co leaching in the system. Adding to this, the excellent catalytic activity exhibited by the catalyst can be ascribed to its hierarchically porous structure, additional active sites and oxygen vacancies (Li et al., 2020).

Pd–Cu, Pd–Ni, Pd–Au and Pd–Ag supported on Mn₃O₄ were used to treat 4-NP solution. Pd–Cu/Mn₃O₄ possessed superior catalytic activity toward the reduction of 4-NP in comparison to the other bimetallic catalysts investigated. This catalyst achieved stable conversion efficiency of 90% after 10 consecutive runs. It was also tested for its feasibility in industrial applications leading to rapid catalysis of simulated wastewater containing 4-NP and good anti-interference toward several inorganic and organic species (Ma et al., 2019). Pt–Rh bimetallic catalyst can also degrade 4-NP to 4-AP in a short period of time with good stability and recyclability (Q. Yan et al., 2020). Bimetallic Hg–Pd catalyst with 1:1 Hg/Pd ratio completely degraded 4-NP to 4-AP in the presence of NaBH₄ retaining its great catalytic performance after five successive cycles (Harika et al., 2020). High stability and great catalytic reducibility were observed in the degradation of p-NP to p-AP using Pd–Pt bimetallic catalyst. The Pd–Pt catalyst achieved improved kinetic apparent rate constants compared to the Pt catalyst (0.5 min⁻¹ vs. 0.2 min⁻¹) (Wang et al., 2019). Mg–Fe Fenton-like catalyst with Mg/Fe of 32:1 exhibited the best performance for the 4-CP degradation achieving complete 4-CP degradation and 91.8% TOC removal (Yang et al., 2019).

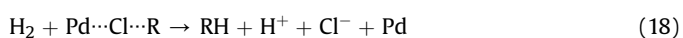
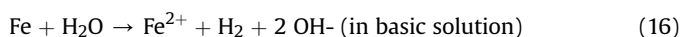
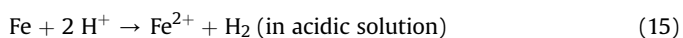
Bimetallic iron–nickel sulfide as peroxydisulfate (PDS) activator was investigated in the removal of 4-CP, 1,4-DCP and 2,4,6-TCP. Fe–

PDS and Ni-PDS systems were employed in the removal of 2,4,6-TCP achieving only 5% and 24%, respectively, indicating inferior catalytic activity compared to Fe–Ni bimetallic catalyst (82%). The results also show that this bimetallic catalyst can efficiently activate PDS to produce sulfate radical ($\text{SO}_4^{\bullet-}$) playing a significant role in the oxidative dechlorination and degradation owing to its strong oxidizing property and the ability for $\bullet\text{OH}$ radical production in basic conditions. This bimetallic catalyst exhibited great catalytic oxidative dechlorination property, PDS activation performance and durability (X. Yan et al., 2020). Various bimetallic catalysts were found to be efficient and effective for the treatment of phenol and its derivatives with a wide range of concentrations.

4.1.4. Chlorinated organic compounds (COCs)

p-dichlorobenzene was completely dechlorinated by Pd–Fe bimetallic reductants with a low catalyst dose of 0.05 g L^{-1} within 3 h at room temperature (Xu et al., 2005a). Similarly, Xu et al. achieved 100% dechlorination efficiency using Pd–Fe catalyst to treat o-dichlorobenzene under similar experimental conditions (Xu et al., 2005b). The Pd–Fe NPs dechlorinated carbon tetrachloride (CT), chloroform (CF), and dichloromethane (DCM) with 65.0%, 67.4%, and 7.0% efficiency, respectively (Wang et al., 2008). Furthermore, Wang et al. used this catalyst to treat the same contaminants, achieving almost complete removal efficiency (90% to > 99%), for CT, CF, and DCM (Wang et al., 2009). These catalysts are also effective for the dechlorination of lindane, tetrachlorobiphenol A, trichloroethene, and tetrachlorethene (Han et al., 2016; Huang et al., 2013, 2009; Nutt et al., 2006).

Furthermore, Pd–Fe catalysts are the most widely used for the dechlorination of various COCs, showing great catalytic efficiency. The reaction mechanisms for the catalytic dechlorination of COCs in acidic and basic media are shown in Fig. 9. The following steps have been proposed: (i) H_2 is generated by the corrosion of iron in water (Eq. (15) and (16)), (ii) RCl, a generalized chlorinated hydrocarbon, is transported to catalyst Pd, simultaneously forming the complex $\text{Pd}\cdots\text{Cl}\cdots\text{R}$ (Eq. (17)), and (iii) RCl is then transformed to the corresponding hydrocarbon RH (Eq. (18)) (Wang et al., 2008).



4.2. Inorganic pollutant treatment

Environmental pollution by nitrates originates mainly from human activities involving excessive long-term use of chemical fertilizers in agriculture, intensive animal husbandry, wastewater and sewage discharge, and landfill leachate (Chiueh et al., 2011). Excessive quantities of nitrate may enter the human body through nitrate-contaminated drinking water or foodstuff. Once they enter the body and are absorbed by it, nitrate can be reduced to nitrite, which may combine with hemoglobin to form methemoglobin, resulting in a serious reduction of the blood oxygen-carrying capacity, which is associated with diseases such as blue baby syndrome. The European Community nitrate limit for both drinking water and wastewater discharge is 50 mg L^{-1} (Barrabés and Sá, 2011).

Hexavalent chromium, Cr(VI), is a highly toxic, mutagenic, and carcinogenic inorganic contaminant classified by the International

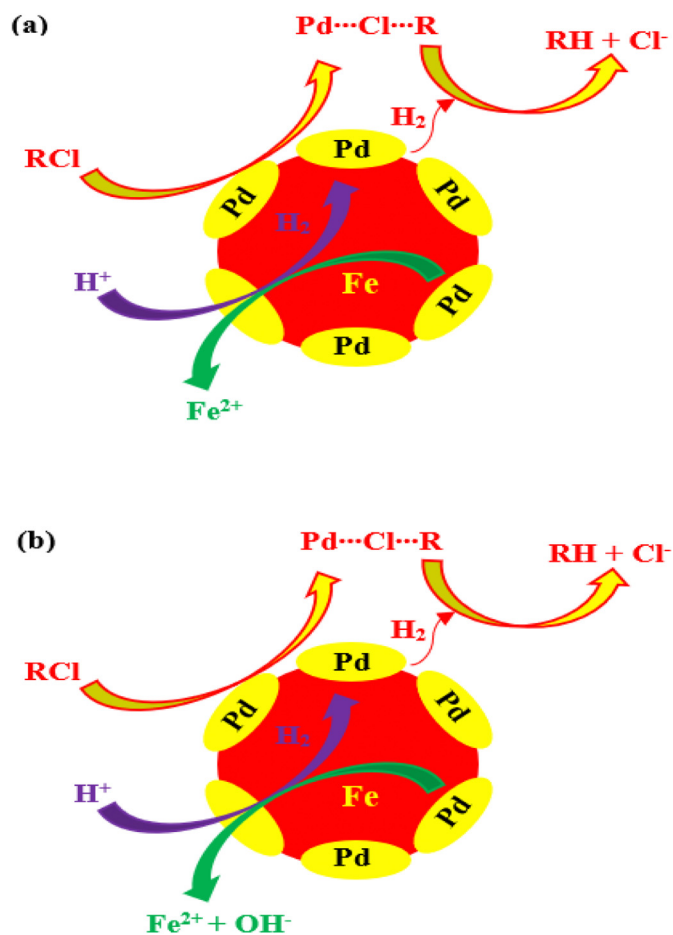


Fig. 9. Reaction mechanism of COC catalytic dechlorination by Pd–Fe bimetallic catalyst in (a) acidic solution and (b) basic solution.

Agency for Research on Cancer as a Class I Carcinogen (Chen et al., 2014; Yao et al., 2018). Water contamination by Cr(VI) is mainly caused by industrial activities including tanning, electroplating, stainless steel manufacturing, wood preservation, and the production of pigments, paints, paper, and pulp (Shi et al., 2019). The WHO limits Cr(VI) in drinking water to 0.05 mg L^{-1} to safeguard human health (Vilela et al., 2019). Moreover, the US EPA set a maximum discharge limit of 0.1 mg L^{-1} to inland surface waters. The Government of India through the Ministry of Environment and Forest also set the minimal national standard to $01. \text{ mg L}^{-1}$ for the safe effluent discharge of Cr(VI) into surface waters (Singh et al., 2011). Consequently, Cr(VI) removal from water and wastewater is very crucial. Cr(III) is less hazardous and less mobile compared to Cr(VI) due to its limited water solubility. It is considered as a nutrient for humans and animals in trace quantities. Therefore, the reduction of Cr(VI) to Cr(III) is a critical step to improve the total chromium removal rate in water and wastewater.

4.2.1. Conventional treatment methods

The removal of nitrates is presently done using reverse osmosis, ion exchange, and electrodialysis. The drawback of these systems is that they remove nitrates and concentrate them in the reject water or brine. The disposal of this rejected water is costly and considered as an environmental issue. Biological denitrification and heterogeneous catalytic systems aim to convert nitrates into harmless nitrogen gas. Biological treatment is proven to be highly effective and efficient for the removal of most pollutants, but biodegradation

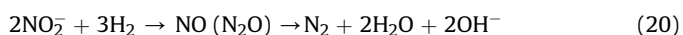
processes are essentially slow and cannot achieve high degrees of removal. Sludge produced by biological treatment increases running costs because of its disposal by either landfilling or burning and consequently causes further environmental issues (Barrabés and Sá, 2011; Fu et al., 2015).

Various conventional methods are used to treat Cr(VI), including adsorption and filtration, chemical precipitation, electrocoagulation, electro-dialysis, ion exchange, and membrane separation (Quiton et al., 2018). However, these technologies have several drawbacks, such as low efficiency, high operating and maintenance cost, sludge generation, which causes disposal issues, and production of secondary pollutants (Alemu et al., 2018). These limit problems applicability in real situations.

4.2.2. Nitrate reduction

Catalytic processes such as denitrification by bimetallic catalysts are promising technologies for converting nitrate (NO_3^-) to harmless nitrogen gas (N_2) in a natural and engineered environment in the presence of a reducing agent (in this case hydrogen).

The catalytic nitrate removal from water has been proposed as an efficient and economical technique for meeting nitrate and nitrite (NO_2^-) standards with no further modifications (Pintar et al., 1998). The nitrate/nitrite hydrogenation process can be described by the following reactions:



NO_3^- is converted to NO_2^- (Eq. (19)), then via an intermediate $\text{NO}/\text{N}_2\text{O}$ to N_2 (Eq. (20)) and the undesired by-product NH_4^+ (Eq. (21)), as shown in Fig. 10(a). The catalytic reduction of NO_3^- using bimetallic catalysts requires a noble metal (M_N) such as Pd, Pt, or Rh, and a promoting transition metal (M_P) such as Cu, Ni, Fe, Sn, or In, as shown in Fig. 10(b). The role of the transition metal is to reduce NO_3^- to NO_2^- according to a redox process, leading to its oxidation.

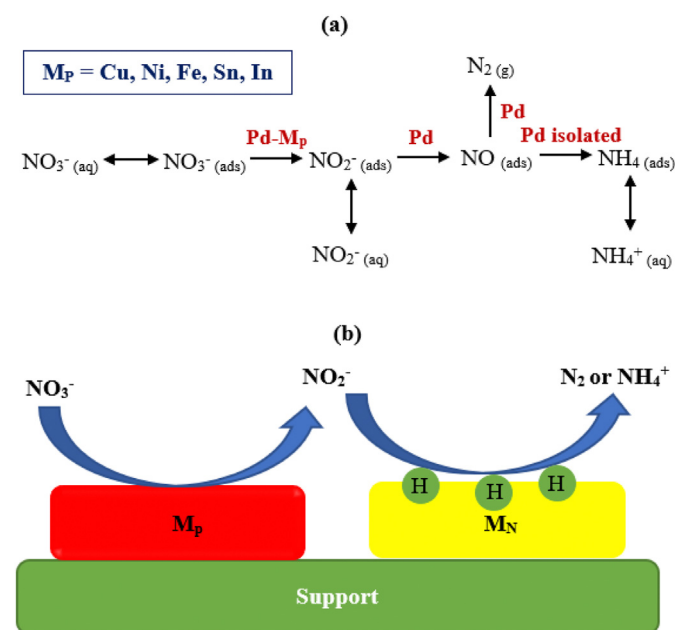


Fig. 10. Denitrification process by (a) Pd- M_P bimetallic catalyst in stepwise mechanism and (b) supported noble metal-promoting transition metal bimetallic catalyst.

Moreover, the role of the noble metal is to stabilize the transition metal in its lower oxidation states by hydrogen spillover (Trawczyński et al., 2011).

NO_3^- was proposed to be reduced to NO_2^- on Pd-Cu centers, and NO_2^- to be reduced on Pd centers, as shown in Fig. 10(a) (Lemaigney et al., 2002). However, not all Pd centers have the same reducing capacity. Pd centers located at the edges and corners of the microcrystals of Pd have a high capacity for hydrogenation, which consequently favors nitrite reduction. Furthermore, N_2 was observed to be mainly formed in the Pd centers located on the terraces of the microcrystals of Pd, because these have a lower hydrogenation capacity (Yoshinaga et al., 2002). The addition of Cu to Pd microcrystals located at the edges and corners deactivates the more reducing Pd and favors selectivity towards N_2 . However, as the Cu content increases, the behavior is reversed and selectivity towards ammonium increases. In this case, Cu is placed on the entire surface of Pd microcrystals and Pd active centers are separated from each other by Cu, and thus nitrite molecules adsorbed on the active centers are also separated, which leads to the formation of ammonia due to the difficulty of recombining the N atoms to form N_2 . In addition, ammonium is formed in Pd centers, thus explaining the increase in selectivity to ammonium as the Pd loading increases (Palomares et al., 2011; Pintar et al., 1998).

In the catalytic reduction of NO_3^- , diverse combinations of metal catalysts and support materials can be utilized. Metallic and non-metallic supports that are eco-friendly, non-toxic, economical, and stable are used as support materials. Metallic support materials include TiO_2 , Al_2O_3 , NZVI, and iron oxide and non-metallic ones include SiO_2 , AC, carbon nanotubes (CNTs), zeolite, and resin. Here, Pd-Cu, Pd-In, Pd-Sn, Pt-Cu, Pt-Sn, Pt-In, Rh-Cu, and Ir-Cu bimetallic catalysts supported on various kinds of materials are discussed and compared in terms of nitrate reduction efficiency and selectivity to nitrogen. Pd-Cu/bentonite completely reduced 100 mg L^{-1} nitrate with 0.64 g L^{-1} catalyst loading at room temperature (Pizarro et al., 2015). Similarly, AC-supported Pd-Cu produced the same result while achieving 98% nitrogen selectivity (Al Bahri et al., 2013). Pd-Cu/pumice was used achieving total nitrate reduction with 91.5% selectivity (Deganello et al., 2000). Total reduction of nitrate and 79% selectivity was also achieved in the presence of H_2 and CO_2 (Sá and Vinek, 2005).

NaY zeolite-supported Pd-Cu catalyst totally reduced 100 mg L^{-1} nitrate with a high N_2 selectivity of 94% with an applied catalyst dosage of 0.5 g L^{-1} . Less than 10% of NO_3^- reduction and less than 80% N_2 selectivity were achieved using Cu/NaY and Pd/NaY showing poor catalytic performance comparing to that of Pd-Cu/NaY catalyst (Soares et al., 2015). With the same amount of catalyst loading, total reduction was achieved using a titania-supported Pd-Cu catalyst. However, the nitrogen selectivity reached only 17%, which does not match that of other Pd-Cu catalysts supported on different materials. Pd supported on CeO_2 , MnO_2 and TiO_2 catalysts gave 47%, 2% and 42% NO_3^- reduction, respectively, indicating that the bimetallic catalyst has greater catalytic activity. The selectivity of Pd-Cu/ TiO_2 was improved (reaching 66%) by adding CNT to the support material (Soares et al., 2011). The catalytic performances of bentonite-supported Pd, Ir, Rh and Pt were compared with Pd-Cu/bentonite and Pd-Sn/bentonite. Both bimetallic catalysts achieved complete reduction of NO_3^- while the monometallic catalysts reached below 63% reduction (Pizarro et al., 2015).

Pd-In catalysts were also observed to be active in the reduction of nitrate. Bentonite- and alumina-supported Pd-In catalysts achieved 100% nitrate reduction with 0.64 and 0.25 g L^{-1} catalyst loading, respectively (Gao et al., 2015; Pizarro et al., 2015). Pd-Sn supported on $\gamma\text{-Al}_2\text{O}_3$, ZSM-5, and zeolite was found to be 100% active for nitrate reduction while achieving 92.4%, 91%, and 88.1%

N₂ selectivity, respectively (Costa et al., 2012; Hamid et al., 2016; Park et al., 2019). Using a different support, similar result for catalytic activity was observed (Pizarro et al., 2015).

A much lower catalytic activity and nitrogen selectivity was reported compared to the results obtained using Pd–Cu supported on AC (Al Bahri et al., 2013; Soares et al., 2010). The choice of support usually affects the activity and selectivity of bimetallic catalysts. In this case, the former used commercial activated carbon (CAC) whereas the latter utilized AC prepared by the chemical activation of grape seeds with phosphoric acid (GS). The significant difference could be caused by the BET surface area. The laboratory-synthesized AC (from grape seeds) shows a higher BET surface area and a significantly high mesoporosity compared to those of the CAC used by Soares et al. (2009). In addition, the GS support was more acidic, which resulted from the groups formed upon the activation of grape seeds with phosphoric acid.

Most of the Pd–Cu based catalysts in the literature led to nitrite formation during the reduction of nitrate. Thus, a support material with a higher concentration of acidic sites such as GS may accelerate the disappearance of nitrite. This agrees with another study showing that the formation of nitrite decreases with pH at pH lower than 3.0 (Centi and Perathoner, 2003). In addition, this species does not appear as a by-product.

The properties of the support material, including its surface area, porosity, and morphology, usually influence the catalytic performance of bimetallic catalysts for catalytic denitrification. The significance of the reactive surface area and porosity of the support has been highlighted (Hao and Zhang, 2017). In this work, Pd–Sn catalysts were supported on various supports such as kaolin–MnO₂, diatomite–kaolin, diatomite–MnO₂, γ -Al₂O₃–kaolin, γ -Al₂O₃–MnO₂, and γ -Al₂O₃–diatomite. Pd–Sn/ γ -Al₂O₃–diatomite was found to exhibit the best catalytic activity and N₂ selectivity among all the catalysts tested due to its high reactive surface area and high porosity, which resulted in well-dispersed metal particles on the catalyst surface.

The effect of support on the nitrate conversion was also studied using Al₂O₃, AC, hydrotalcite, and graphite (Palomares et al., 2011). For the Pd–Cu catalysts tested, the alumina-supported catalyst gave the highest catalytic activity, reaching about 95% for 8 h. Similarly, the hydrotalcite and graphite-supported catalysts reached remarkably lower activity, with 45% and 35% conversion for 7 h. Notable differences were also observed with five types of support material. The degree of catalytic activity was found to follow the order Pd–Cu/CeO₂ > Pd–Cu/ZrO₂ > Pd–Cu/TiO₂ > Pd–Cu/SiO₂ and Pd–Cu/Al₂O₃ under the same experimental conditions (Wada et al., 2012).

Moreover, 99.5%, 63%, and 43% nitrate reduction were achieved using Pd–Cu supported on maghemite, hematite, and alumina, respectively (Jung et al., 2012). TiO₂-supported Pd–Cu catalyst was found to have the highest catalytic activity among the support materials studies (Soares et al., 2011). These include CeO₂, CeO, MnO₂, Al₂O₃, SiO₂, CAC, CNT, AC–cerium oxide composite, and AC–manganese oxide composite. Although the same promoting transition metals and noble metals were used for the catalytic nitrate reduction, different performances in terms of activity and selectivity were achieved by various support materials, which shows that the support greatly affects catalytic activity and selectivity for the catalytic reduction of nitrate.

The loading of promoting transition metals and noble metals also plays an important role in effective nitrate reduction, which affects the metal ratio. The nitrate reduction efficiency was found to follow a volcano shape with increased promotion transition metal (M_P) loading (Gao et al., 2015; Jung et al., 2012). It was observed that as the Pd:In ratio increased for a constant amount of Pd, the reaction rate constant decreased by almost half due to the low In

content in the Pd–In/Al₂O₃ catalyst (Gao et al., 2015). The reduction efficiency was observed by Jung et al. to increase with an increase in M_P loading because M_P usually reduces NO₃[−] to NO₂[−], as discussed above (Jung et al., 2012).

When Cu was in excess, there was a notable decrease in the NO₃[−] reduction, going from 96.6% (1.6 wt%) to 93.6% and 86.1% for 2.2 wt% and 2.8 wt%, respectively (Jung et al., 2014). It should be noted that there was an increase in reactivity due to the increased number of available M_P sites for NO₃[−] reduction. However, excess M_P can lower the number of reactive sites for a noble metal (M_N).

M_N loading greatly influences the reaction because M_N reduces NO₂[−] to N₂ or NH₄⁺ when H₂ is present and regenerates oxidized M_P. The effect of M_N loading is similar to have of M_P. The reduction of nitrate follows a volcano shape with an increase in metal loading.

It was reported that reduction efficiency increased from 75% to 100% as the Pd concentration was increased from 1 to 5 wt% in 2.5% Pd–Cu/AC catalyst (Al Bahri et al., 2013). Pd concentration can also affect the production of N₂ and NH₄⁺ as final products. It was reported that NO₂[−] production dropped to 0% while NH₄⁺ production increased from 30.4% to 38.7% as the Pd content was increased from 0.4 to 2.8 wt% in a Pd–Cu catalyst supported on hematite (Jung et al., 2014). Optimal loading of noble metal should be determined for efficient catalytic NO₃[−] reduction.

The influence of metal loading also highly depends on experimental conditions and the type of catalyst used. It was observed that the choice of M_N also affects the reduction efficiency. Soares et al. used Pd, Pt, Rh, and Ir as noble metals together with Cu as the promoter metal supported on AC (Soares et al., 2009). Their study showed 63%, 56%, 98%, and 55% reduction for Pd–Cu, Pt–Cu, Rh–Cu, and Ir–Cu catalysts, respectively, for a noble metal to Cu ratio of about 1.0. It should be noted that there is no linear relationship between reduction efficiency, reduction rate, and N₂ selectivity and the metal loading on the surface of the catalyst. Moreover, the effect of metal loading follows a volcano shape, which indicates that a balance between M_P and M_N sites should be achieved for fast and selective NO₃[−] reduction.

Pd–Sn/zeolite achieved complete nitrate removal and 88.1% nitrogen selectivity. This result can be ascribed to the high surface area and stability of the zeolite phase (Park et al., 2019). Similarly, kaolinite-supported Pd–Sn exhibited complete NO₃[−] removal with fast reduction kinetics and 71% selectivity toward N₂ during batch reactions. During continuous tests, 100% NO₃[−] removal and 80% N₂ selectivity were observed for 60 h. The Pd–Sn/kaolinite catalyst had a superior reaction kinetics and operational durability ascribing to the negligible metal leaching from catalyst surface and the stability of the catalyst structure (Hamid et al., 2016). Pd–In supported on polymer fibres showed better N₂ selectivity and catalyst stability in the NO₃[−] reduction compared with Pd–In catalysts synthesized on inorganic supports (SiO₂, Al₂O₃ and carbon fibers) (Marchesini et al., 2020).

Pd–Cu catalyst was found to be the most active and selective in the transformation of nitrate to nitrogen among the bimetallic catalysts discussed in this review. It is thus widely studied for catalytic nitrate reduction.

4.2.3. Hexavalent chromium reduction

Recently, Fe-based bimetallic catalysts have been applied for the reduction of Cr(VI) to Cr(III). Few studies have been conducted on their catalytic performance on Cr(VI) reduction. Fe–Pd-immobilized polyethyleneimine filter paper catalyst was synthesized for the catalytic reduction of Cr(VI), showing high efficiency and outstanding catalytic reusability (Shi et al., 2019). 97.4%, 98.6%, and 99.4% of Cr(VI) was reduced to Cr(III) within 28 min of reaction time for the first, second, and third cycles, respectively (Shi et al., 2019). It is interesting that the catalytic reduction efficiency of the

bimetallic filter paper slightly increased when the catalytic cycle number increased. This phenomenon may be due to the production of more dissociated hydrogen from the H_2 in the lattice of the Pd layer to support the powerful reduction process. Furthermore, the stability of the catalyst was assessed during repeated catalytic reduction. Similarly, Fe–Ni supported on montmorillonite (MMT) clay was used, achieving almost complete (>99%) reduction within 10 min at pH of 1–3, suggesting high catalytic reduction efficiency. The Cr(VI) reduction rate was observed to decrease with increasing pH, indicating that optimal Cr(VI) reduction occurs under acidic conditions. As pH decreases, H^+ concentration increases, resulting in increased nickel hydride formation, hence increasing reduction efficiency (Kadu et al., 2011).

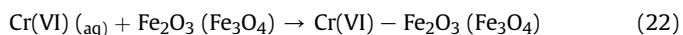
A decrease in efficiency can result from the formation of hydroxide and oxide layers on the NP surface, hindering the electron flow toward Cr(VI). Incorporating Fe and Ni NPs into the MMT clay matrix ensured the proper dispersion of the NPs and the removal capacity was enhanced, combining the reduction capacity of the Fe–Ni NPs and the adsorption tendency of MMT. The Fe–Ni catalyst prepared by in situ syntheses also showed great reusability (~100%) after 3 cycles (Kadu et al., 2011).

Moreover, an ultrasound-assisted Fe–Ni bimetallic system reached 94.7% reduction efficiency within 10 min (Zhou et al., 2016). The Fe–Ni NPs showed good reusability and good catalytic performance under ultrasound irradiation even after 26 d of aging at pH 5 (Zhou et al., 2016). The synthesized Fe–Ni NPs demonstrated good reduction performance for the removal of Cr(VI) at acidic pH because the reactive H^\bullet species that are mediated by the Ni catalyst increase as H^+ increases (Zhou et al., 2014). The presence of Cl^- and NO_3^- , even as high as 400 mg L^{-1} , did not affect Cr(VI) reduction by Fe–Ni NPs, which maintained >98% efficiency.

An MOF, ZIF-8, was used as a support material for Pd–Cu bimetallic alloy NPs for the photoreduction of Cr(VI). The as-prepared catalyst possessed excellent photoreduction activity for Cr(VI) reduction compared to that of its monometallic counterparts and unsupported catalysts. The catalytic performances are as follows: Pd–Cu/ZIF-8 > Cu/ZIF-8 > Pd/ZIF-8 > Pd–Cu NPs > Pd NPs > Cu NPs > ZIF-8 (Zhang and Park, 2019). Bimetallic Sn–Zn oxysulfide nanocatalyst achieved 100% photocatalytic reduction efficiency under visible light at room temperature within 80 min showing excellent efficiency compared to Zn monometallic catalyst (<20%) (Zelekew et al., 2019). Fe–Al BNP exhibited a high catalytic activity and stability in the treatment of Cr(VI)-contaminated groundwater remediation. The mechanisms for the removal of Cr(VI) included reduction, precipitation and adsorption (Ou et al., 2020). Fe–Cu/chitosan possessed dual functions including the catalytic degradation of Cr(III)-organic complexes and efficient inhibition of Cr(VI) accumulation (Shen et al., 2020). Bimetallic Fe–In catalyst achieved improved photocatalytic activity for the reduction of Cr(VI) under visible light illumination which outperformed 3.4 times higher than that of the monometallic In catalyst under identical conditions (S. Wang et al., 2020).

The proposed mechanism for the entire process of Cr(VI) reduction on the Fe–Ni bimetallic catalyst surface is shown in Fig. 11 (Zhou et al., 2014). It includes:

(a) Cr(VI) adsorption by iron oxide on the Fe–Ni catalyst surface



(b) Cr(VI) reduction to Cr(III) via reactive H^\bullet species catalyzed by Ni

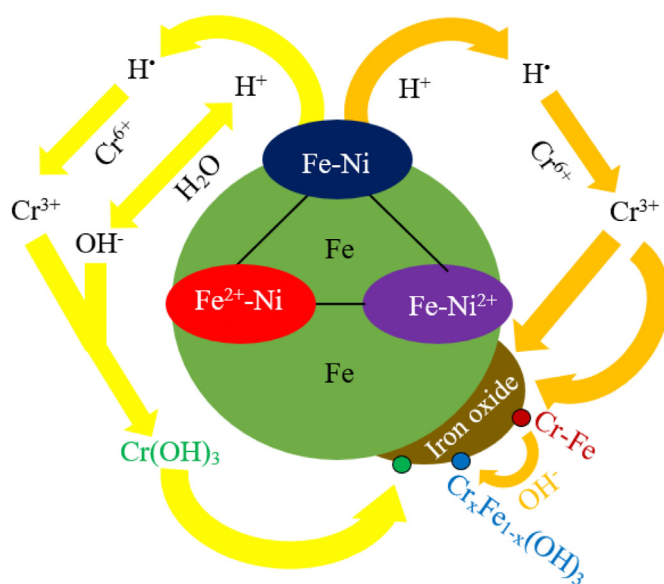
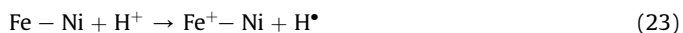
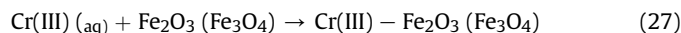


Fig. 11. Mechanistic pathway of Cr(VI) reduction by Ni–Fe bimetallic catalyst.



(c) Cr(III) adsorption on iron oxide surface together with the formation of Cr(OH)_3 and co-precipitation of $\text{Cr}_x\text{Fe}_{1-x}(\text{OH})_3$



Cr(VI) reduction and adsorption occur simultaneously on the surface of the composite. The nickel catalyst in the Fe–Ni NPs not only inhibits the passivation of iron but also facilitates the efficient flow of electrons from iron (electron donor) to Cr(VI) (electron acceptor) mediated by the nickel site acting as an electron shuttle between the electron donor and acceptor (Zhou et al., 2014).

5. Remarks and conclusions

There has been great interest in the synthesis and use of diverse bimetallic catalysts for the removal of various environmental contaminants. Improvements in removal efficiencies have been extensively reported. This review gives an overview of existing synthesis techniques and applications of bimetallic catalysts in water and wastewater remediation.

The catalytic properties of bimetallic catalysts highly depend on their shape, size, structure, composition, and surface properties, which are greatly influenced by the synthesis method. Chemical methods are the most widely used techniques for the synthesis of these catalysts. However, chemical methods often have disadvantages related to the presence of toxic solvents and reducing agents. Co-precipitation is a widely used synthesis method. The addition of dispersing agents and stabilizers can avoid the disadvantages of agglomeration during preparation. Deposition precipitation provides easy control of particle size and composition. However, impurities may precipitate together with the target product. Plasma technology is a single-step process for bimetallic catalyst synthesis.

The sol-gel technique is a simple and inexpensive method with excellent microstructural control, superior homogeneity and purity at the molecular level, good thermal stability of supported metals, and low crystallization temperature. This method requires calcination as a post-treatment, similar to the impregnation technique. Reverse micelle synthesis leads to narrow particle size distributions, negligible contamination of the product during homogenization of starting compounds, low energy consumption, low aging times, use of simple equipment, and improved control of particle size, shape, uniformity, and dispersity.

Summing up, present synthesis techniques for bimetallic systems are often complex and costly. Thus, future research should attempt to decrease the preparation cost by searching for and testing new low-cost raw materials and developing simpler and more practical methods. Iron-based bimetallic catalysts are a great addition to the more established noble and transition-metal-based systems. They are an attractive system for further study and development due to the easily interchangeable oxidation states of Fe²⁺ to Fe³⁺, high selectivity, relatively low toxicity, and low cost.

The application of bimetallic systems in the field of heterogeneous catalysis for the remediation of organic and inorganic contaminants has achieved remarkable success. However, the roles and performances of these catalysts in the removal of these pollutants are different. In bimetallic catalysts, a substrate metal and a second metal are combined to serve as a feasible alternative dichlorination and hydrogenation reagent that can also store active hydrogen species. These catalysts have remarkable catalytic properties and function, which makes them good catalysts for the removal of dyes, degradation of phenol and its derivatives, and dechlorination of COCs. Considering the high reducibility of these catalysts, they are also utilized as reductants for the removal of NO₃⁻ and Cr(VI).

Declaration of competing interest

The authors declare that they have no known competing financial interests or personal relationships that could have appeared to influence the work reported in this paper.

Acknowledgements

The authors are grateful to the Ministry of Science and Technology, Taiwan (MOST 107-2221-E-041-001-MY3 and MOST 106-2622-E006-037-CC2) for the financial support with this work. Special thanks to Engr. Carl Francis Lacson and Ma. Antonette Rubios for their honest and helpful comments and suggestions during the course of this work.

References

Aftab, T.B., Hussain, A., Li, D., 2019. Application of a novel bimetallic hydrogel based on iron and cobalt for the synergistic catalytic degradation of Congo Red dye. *J. Chin. Chem. Soc.* 66, 919–927. <https://doi.org/10.1002/jccs.201800388>.

Ahmed, Y., Yaakob, Z., Akhtar, P., 2016. Degradation and mineralization of methylene blue using a heterogeneous photo-Fenton catalyst under visible and solar light irradiation. *Catal. Sci. Technol.* 6, 1222–1232. <https://doi.org/10.1039/c5cy01494h>.

Al-Khalid, T., El-Naas, M.H., 2012. Aerobic biodegradation of phenols: a comprehensive review. *Crit. Rev. Environ. Sci. Technol.* 42, 1631–1690. <https://doi.org/10.1080/10643389.2011.569872>.

Al Bahri, M., Calvo, L., Gilarranz, M.A., Rodriguez, J.J., Epron, F., 2013. Activated carbon supported metal catalysts for reduction of nitrate in water with high selectivity towards N₂. *Appl. Catal. B Environ.* 138–139, 141–148. <https://doi.org/10.1016/j.apcatb.2013.02.048>.

Alemu, A., Lemma, B., Gabbiye, N., Tadele, M., Teferi, M., 2018. Removal of chromium (VI) from aqueous solution using vesicular basalt: a potential low cost wastewater treatment system. *Heliyon* 4, e00682. <https://doi.org/10.1016/j.heliyon.2018.e00682>.

Ali, S., Mohd Zabidi, N.A., Subbarao, D., 2012. Synthesis and characterization of bimetallic Fe/Co nanocatalyst on CNTs for Fischer-Tropsch reaction. *J. Nano Res.* 16, 9–14. <https://dx.doi.org/10.4028/www.scientific.net/JNanoR.16.9>.

Aluha, J., Abatzoglou, N., 2017. Promotional effect of Mo and Ni in plasma-synthesized Co-Fe/C bimetallic nano-catalysts for Fischer-Tropsch synthesis. *J. Ind. Eng. Chem.* 50, 199–212. <https://doi.org/10.1016/j.jiec.2017.02.018>.

Aluha, J., Bere, K., Abatzoglou, N., Gitzhofer, F., 2016. Synthesis of nano-catalysts by induction suspension plasma technology (SPS) for Fischer-Tropsch reaction. *Plasma Chem. Plasma Process.* 36, 1325–1348. <https://doi.org/10.1007/s11090-016-9734-1>.

Balachandran, S., Swaminathan, M., 2012. Superior photocatalytic activity of bimetallic Cd-Ag-ZnO for the degradation of azo dyes under UV light. *Emerg. Mater. Res.* 1, 157–163. <https://doi.org/10.1680/emr.11.00025>.

Barrabés, N., Sá, J., 2011. Catalytic nitrate removal from water, past, present and future perspectives. *Appl. Catal. B Environ.* 104, 1–5. <https://doi.org/10.1016/j.apcatb.2011.03.011>.

Bokare, A.D., Chikate, R.C., Rode, C.V., Paknikar, K.M., 2008. Iron-nickel bimetallic nanoparticles for reductive degradation of azo dye Orange G in aqueous solution. *Appl. Catal. B Environ.* 79, 270–278. <https://doi.org/10.1016/j.apcatb.2007.10.033>.

Bokare, A.D., Chikate, R.C., Rode, C.V., Paknikar, K.M., 2007. Effect of surface chemistry of Fe-Ni nanoparticles on mechanistic pathways of azo dye degradation. *Environ. Sci. Technol.* 41, 7437–7443. <https://doi.org/10.1021/es071107q>.

Broholm, K., Christensen, T.H., Jensen, B.K., 1993. Different abilities of eight mixed cultures of methane-oxidizing bacteria to degrade TCE. *Water Res.* 27, 215–224. [https://doi.org/10.1016/0043-1354\(93\)90078-V](https://doi.org/10.1016/0043-1354(93)90078-V).

Cai, C., Zhang, H., Zhong, X., Hou, L., 2015. Ultrasound enhanced heterogeneous activation of peroxymonosulfate by a bimetallic Fe-Co/SBA-15 catalyst for the degradation of Orange II in water. *J. Hazard Mater.* 283, 70–79. <https://doi.org/10.1016/j.jhazmat.2014.08.053>.

Centi, G., Perathoner, S., 2003. Remediation of water contamination using catalytic technologies. *Appl. Catal. B Environ.* 41, 15–29. [https://doi.org/10.1016/S0926-3373\(02\)00198-4](https://doi.org/10.1016/S0926-3373(02)00198-4).

Chen, L., Jiang, X., Xie, R., Zhang, Y., Jin, Y., Jiang, W., 2020. A novel porous biochar-supported Fe-Mn composite as a persulfate activator for the removal of acid red 88. *Separ. Purif. Technol.* 250, 117232. <https://doi.org/10.1016/j.seppur.2020.117232>.

Chen, S.S., Huang, Y.C., Chen, T.Y., 2014. Reduction of hexavalent chromium in water using iron-aluminum bimetallic particles. *Adv. Mater. Res.* 849, 142–146. <https://dx.doi.org/10.4028/www.scientific.net/AMR.849.142>.

Chiueh, P. T., Lee, Y.H., Su, C.Y., Lo, S.L., 2011. Assessing the environmental impact of five Pd-based catalytic technologies in removing of nitrates. *J. Hazard Mater.* 192, 837–845. <https://doi.org/10.1016/j.jhazmat.2011.05.096>.

Costa, A.O., Ferreira, L.S., Passos, F.B., Maia, M.P., Peixoto, F.C., 2012. Microkinetic modeling of the hydrogenation of nitrate in water on Pd-Sn/Al₂O₃ catalyst. *Appl. Catal. Gen.* 445–446, 26–34. <https://doi.org/10.1016/j.apcata.2012.07.043>.

Cybula, A., Nowaczyk, G., Jarek, M., Zaleska, A., 2014. Preparation and characterization of Au/Pd Modified-TiO₂ photocatalysts for phenol and toluene degradation under visible light - the effect of calcination temperature. *J. Nanomater.* <https://doi.org/10.1155/2014/918607>.

Dai, C., Zhang, A., Luo, L., Zhang, X., Liu, M., Wang, J., Guo, X., Song, C., 2017. Hollow zeolite-encapsulated Fe-Cu bimetallic catalysts for phenol degradation. *Catal. Today* 297, 335–343. <https://doi.org/10.1016/j.cattod.2017.02.001>.

Deganello, F., Liotta, L.F., Macaluso, A., Venezia, A.M., Deganello, G., 2000. Catalytic reduction of nitrates and nitrites in water solution on pumice-supported Pd-Cu catalysts. *Appl. Catal. B Environ.* 24, 265–273. [https://doi.org/10.1016/S0926-3373\(99\)00109-5](https://doi.org/10.1016/S0926-3373(99)00109-5).

Deraz, N.M., 2018. The comparative jurisprudence of catalysts preparation methods: I. precipitation and impregnation methods. *J. Ind. Eng. Chem.* 2, 19–21.

Dong, Y., Han, Z., Dong, S., Wu, J., Ding, Z., 2011. Enhanced catalytic activity of Fe bimetallic modified PAN fiber complexes prepared with different assisted metal ions for degradation of organic dye. *Catal. Today* 175, 299–309. <https://doi.org/10.1016/j.cattod.2011.04.026>.

Duarte, F., Maldonado-Hódar, F.J., Pérez-Cadenas, A.F., Madeira, L.M., 2009. Fenton-like degradation of azo-dye Orange II catalyzed by transition metals on carbon aerogels. *Appl. Catal. B Environ.* 85, 139–147. <https://doi.org/10.1016/j.apcatb.2008.07.006>.

Dükkancı, M., Gündüz, G., Yılmaz, S., Yaman, Y.C., Prikhod'ko, R.V., Stolyarova, I.V., 2010. Characterization and catalytic activity of CuFeZSM-5 catalysts for oxidative degradation of Rhodamine 6G in aqueous solutions. *Appl. Catal. B Environ.* 95, 270–278. <https://doi.org/10.1016/j.apcatb.2010.01.004>.

Duvenhage, D.J., Coville, N.J., 2005. Fe:Co/TiO₂ bimetallic catalysts for the Fischer-Tropsch reaction: Part 3: the effect of Fe:Co ratio, mixing and loading on FT product selectivity. *Appl. Catal. Gen.* 289, 231–239. <https://doi.org/10.1016/j.apcata.2005.05.008>.

Dvorak, B.I., Lawler, D.F., Speitel, G.E., Jones, D.L., Boadway, D.A., 1993. Selecting among physical/chemical processes for removing synthetic organics from water. *Water Environ. Res.* 65, 827–838. <https://doi.org/10.2175/wer.65.7.4>.

Ezzatahmedi, N., Bao, T., Liu, H., Millar, G.J., Ayoko, G.A., Zhu, J., Zhu, R., Liang, X., He, H., Xi, Y., 2018. Catalytic degradation of Orange II in aqueous solution using diatomite-supported bimetallic Fe/Ni nanoparticles. *RSC Adv.* 8, 7687–7696. <https://doi.org/10.1039/c7ra13348k>.

Ezzatahmedi, N., Marshall, D.L., Hou, K., Ayoko, G.A., Millar, G.J., Xi, Y., 2019a. Simultaneous adsorption and degradation of 2,4-dichlorophenol on sepiolite-supported bimetallic Fe/Ni nanoparticles. *J. Environ. Chem. Eng.* 7, 102955. <https://doi.org/10.1016/j.jece.2019.102955>.

Ezzatahmedi, N., Millar, G.J., Ayoko, G.A., Zhu, J., Zhu, R., Liang, X., He, H., Xi, Y., 2019b. Degradation of 2,4-dichlorophenol using palygorskite-supported

- bimetallic Fe/Ni nanocomposite as a heterogeneous catalyst. *Appl. Clay Sci.* 168, 276–286. <https://doi.org/10.1016/j.clay.2018.11.030>.
- Fang, L., Xu, C., Zhang, W., Huang, L.Z., 2018. The important role of polyvinylpyrrolidone and Cu on enhancing dechlorination of 2,4-dichlorophenol by Cu/Fe nanoparticles: performance and mechanism study. *Appl. Surf. Sci.* 435, 55–64. <https://doi.org/10.1016/j.apsusc.2017.11.084>.
- Foster, S.L., Estoque, K., Voecks, M., Rentz, N., Greenlee, L.F., 2019. Removal of synthetic azo dye using bimetallic nickel-iron nanoparticles. *J. Nanomater.* <https://doi.org/10.1155/2019/9807605>.
- Fu, F., Cheng, Z., Lu, J., 2015. Synthesis and use of bimetallic and bimetal oxides in contaminants removal from water: a review. *RSC Adv.* 5, 85395–85409. <https://doi.org/10.1039/c5ra13067k>.
- Fu, M., Li, C., Lu, P., Qu, L., Zhang, M., Zhou, Y., Yu, M., Fang, Y., 2014. A review on selective catalytic reduction of NO_x by supported catalysts at 100–300°C - catalysts, mechanism, kinetics. *Catal. Sci. Technol.* 4, 14–25. <https://doi.org/10.1039/c3cy00414g>.
- Gao, Z., Zhang, Yonggang, Li, D., Werth, C.J., Zhang, Yalei, Zhou, X., 2015. Highly active Pd-In/mesoporous alumina catalyst for nitrate reduction. *J. Hazard Mater.* 286, 425–431. <https://doi.org/10.1016/j.jhazmat.2015.01.005>.
- Garrido-Ramírez, E.G., Marco, J.F., Escalona, N., Ureta-Zañartu, M.S., 2016. Preparation and characterization of bimetallic Fe-Cu allophane nanoclays and their activity in the phenol oxidation by heterogeneous electro-Fenton reaction. *Microporous Mesoporous Mater.* 225, 303–311. <https://doi.org/10.1016/j.micromeso.2016.01.013>.
- Ghughe, S.P., Saroha, A.K., 2018. Catalytic ozonation of dye industry effluent using mesoporous bimetallic Ru-Cu/SBA-15 catalyst. *Process Saf. Environ. Protect.* 118, 125–132. <https://doi.org/10.1016/j.psep.2018.06.033>.
- Gonzalez, R.D., Lopez, T., Gomez, R., 1997. Sol-gel preparation of supported metal catalysts. *Catal. Today* 35, 293–317. [https://doi.org/10.1016/S0920-5861\(96\)00162-9](https://doi.org/10.1016/S0920-5861(96)00162-9).
- Guo, Y., Zelekew, O.A., Sun, H., Kuo, D.H., Lin, J., Chen, X., 2020. Catalytic reduction of organic and hexavalent chromium pollutants with highly active bimetal CuBiOS oxysulfide catalyst under dark. *Separ. Purif. Technol.* 242, 116769. <https://doi.org/10.1016/j.seppur.2020.116769>.
- Hai, Z., El Kolli, N., Uribe, D.B., Beaunier, P., José-Yacamán, M., Vigneron, J., Etcheberry, A., Sorgues, S., Colbeau-Justin, C., Chen, J., Remita, H., 2013. Modification of TiO₂ by bimetallic Au-Cu nanoparticles for wastewater treatment. *J. Mater. Chem. A*, 1, 10829–10835. <https://doi.org/10.1039/c3ta11684k>.
- Hameed, S.A., 2016. Photo-degradation of Vat dye by bimetallic photo-catalysts (Cu-Ni/TiO₂ and Cu-Ni/zno) under UV and visible light sources. *IOSR J. Environ. Sci.* 10 <https://doi.org/10.9790/2402-1004020105>.
- Hamid, S., Kumar, M.A., Lee, W., 2016. Highly reactive and selective Sn-Pd bimetallic catalyst supported by nanocrystalline ZSM-5 for aqueous nitrate reduction. *Appl. Catal. B Environ.* 187, 37–46. <https://doi.org/10.1016/j.apcatb.2016.01.035>.
- Han, Y., Liu, C., Horita, J., Yan, W., 2016. Trichloroethene hydrodechlorination by Pd-Fe bimetallic nanoparticles: solute-induced catalyst deactivation analyzed by carbon isotope fractionation. *Appl. Catal. B Environ.* 188, 77–86. <https://doi.org/10.1016/j.apcatb.2016.01.047>.
- Hao, L., Huiping, D., Jun, S., 2012. Activated carbon and cerium supported on activated carbon applied to the catalytic ozonation of polycyclic aromatic hydrocarbons. *J. Mol. Catal. Chem.* 363–364. <https://doi.org/10.1016/j.molcata.2012.05.022>.
- Hao, S., Zhang, H., 2017. High catalytic performance of nitrate reduction by synergistic effect of zero-valent iron (Fe⁰) and bimetallic composite carrier catalyst. *J. Clean. Prod.* 167, 192–200. <https://doi.org/10.1016/j.jclepro.2017.07.255>.
- Harika, V.K., Sadhanala, H.K., Perelshtein, I., Gedanken, A., 2020. Sonication-assisted synthesis of bimetallic Hg/Pd alloy nanoparticles for catalytic reduction of nitrophenol and its derivatives. *Ultrason. Sonochem.* 60, 104804. <https://doi.org/10.1016/j.ultrasonch.2019.104804>.
- Hu, L., Zhang, G., Liu, M., Wang, Q., Dong, S., Wang, P., 2019. Application of nickel foam-supported Co₃O₄-Bi₂O₃ as a heterogeneous catalyst for BPA removal by peroxymonosulfate activation. *Sci. Total Environ.* 647, 352–361. <https://doi.org/10.1016/j.scitotenv.2018.08.003>.
- Huang, L., Zhang, L., Li, D., Xin, Q., Jiao, R., Hou, X., Zhang, Y., Li, H., 2020. Enhanced phenol degradation at near neutral pH achieved by core-shell hierarchical 4A zeolite/Fe@Cu catalyst. *J. Environ. Chem. Eng.* 8, 103933. <https://doi.org/10.1016/j.jece.2020.103933>.
- Huang, Q., Liu, W., Peng, P., Huang, W., 2013. Reductive dechlorination of tetrachlorobisphenol A by Pd/Fe bimetallic catalysts. *J. Hazard Mater.* 262, 634–641. <https://doi.org/10.1016/j.jhazmat.2013.09.015>.
- Huang, Y., Liu, F., Li, D., 2009. Degradation of tetrachloromethane and tetrachloroethene by Ni/Fe bimetallic nanoparticles. *J. Phys. Conf. Ser.* 188 <https://doi.org/10.1088/1742-6596/188/1/012014>.
- Ismagilov, Z.R., Podyacheva, O.Y., Solonenko, O.P., Pushkarev, V.V., Kuz'min, V.I., Ushakov, V.A., Rudina, N.A., 1999. Application of plasma spraying in the preparation of metal-supported catalysts. *Catal. Today* 51, 411–417. [https://doi.org/10.1016/S0920-5861\(99\)00030-9](https://doi.org/10.1016/S0920-5861(99)00030-9).
- Ismail, M., Khan, M.I., Khan, S.B., Khan, M.A., Akhtar, K., Asiri, A.M., 2018. Green synthesis of plant supported Cu-Ag and Cu-Ni bimetallic nanoparticles in the reduction of nitrophenols and organic dyes for water treatment. *J. Mol. Liq.* 260, 78–91. <https://doi.org/10.1016/j.molliq.2018.03.058>.
- Jadhav, D.N., Vanjara, A.K., 2004. Removal of phenol from wastewater using sawdust, polymerized sawdust and sawdust carbon. *Indian J. Chem. Technol.* 11, 35–41.
- Jiang, S., Zhang, H., Yan, Y., Zhang, X., 2017. Preparation and characterization of porous Fe-Cu mixed oxides modified ZSM-5 coating/PSSF for continuous degradation of phenol wastewater. *Microporous Mesoporous Mater.* 240, 108–116. <https://doi.org/10.1016/j.micromeso.2016.11.020>.
- Jovanovic, G.N., Plazl, P.Z., Sakrithichai, P., Al-Khaldi, K., 2005. Dechlorination of p-chlorophenol in a microreactor with bimetallic Pd/Fe catalyst. *Ind. Eng. Chem. Res.* 44, 5099–5106. <https://doi.org/10.1021/ie049496+>.
- Jung, J., Bae, S., Lee, W., 2012. Nitrate reduction by maghemite supported Cu-Pd bimetallic catalyst. *Appl. Catal. B Environ.* 127, 148–158. <https://doi.org/10.1016/j.apcatb.2012.08.017>.
- Jung, S., Bae, S., Lee, W., 2014. Development of Pd-Cu/hematite catalyst for selective nitrate reduction. *Environ. Sci. Technol.* 48, 9651–9658. <https://doi.org/10.1021/es502263p>.
- Kadu, B.S., Sathre, Y.D., Ingle, A.B., Chikate, R.C., Patil, K.R., Rode, C.V., 2011. Efficiency and recycling capability of montmorillonite supported Fe-Ni bimetallic nanocomposites towards hexavalent chromium remediation. *Appl. Catal. B Environ.* 104, 407–414. <https://doi.org/10.1016/j.apcatb.2011.02.011>.
- Khan, A., Liao, Z., Liu, Y., Jawad, A., Iftikhar, J., Chen, Z., 2017. Synergistic degradation of phenols using peroxymonosulfate activated by CuO-Co₃O₄/MnO₂ nanocatalyst. *J. Hazard Mater.* 329, 262–271. <https://doi.org/10.1016/j.jhazmat.2017.01.029>.
- Kim, H.H., Teramoto, Y., Ogata, A., Takagi, H., Nanba, T., 2016. Plasma catalysis for environmental treatment and energy applications. *Plasma Chem. Plasma Process.* 36, 45–72. <https://doi.org/10.1007/s11090-015-9652-7>.
- Kim, P., Kim, Y., Kang, T., Song, I.K., Yi, J., 2007. Preparation of nickel-mesoporous materials and their application to the hydrodechlorination of chlorinated organic compounds. *Catal. Surv. Asia* 11, 49–58. <https://doi.org/10.1007/s10563-007-9017-1>.
- Kizling, M.B., Järås, S.G., 1996. A review of the use of plasma techniques in catalyst preparation and catalytic reactions. *Appl. Catal. Gen.* 147, 1–21. [https://doi.org/10.1016/S0926-860X\(96\)00215-3](https://doi.org/10.1016/S0926-860X(96)00215-3).
- Lai, B., Zhang, Y., Chen, Z., Yang, P., Zhou, Y., Wang, J., 2014. Removal of p-nitrophenol (PNP) in aqueous solution by the micron-scale iron-copper (Fe/Cu) bimetallic particles. *Appl. Catal. B Environ.* 144, 816–830. <https://doi.org/10.1016/j.apcatb.2013.08.020>.
- Lavanya, C., Dhankar, R., Chhikara, S., Sheoran, S., 2014. Review article degradation of toxic dyes : a review. *Int. J. Curr. Microbiol. Appl. Sci.* 3, 189–199.
- Lee, D.K., Cho, I.C., Lee, G.S., Kim, S.C., Kim, D.S., Yang, Y.K., 2004. Catalytic wet oxidation of reactive dyes with H₂O₂ mixture on Pd-Pt/Al₂O₃ catalysts. *Separ. Purif. Technol.* 34, 43–50. [https://doi.org/10.1016/S1383-5866\(03\)00173-4](https://doi.org/10.1016/S1383-5866(03)00173-4).
- Lemaignen, L., Tong, C., Begon, V., Burch, R., Chadwick, D., 2002. Catalytic denitrification of water with palladium-based catalysts supported on activated carbons. *Catal. Today* 75, 43–48. [https://doi.org/10.1016/S0920-5861\(02\)00042-1](https://doi.org/10.1016/S0920-5861(02)00042-1).
- Li, A., Shen, K., Chen, J., Li, Z., Li, Y., 2017. Highly selective hydrogenation of phenol to cyclohexanol over MOF-derived non-noble Co-Ni@NC catalysts. *Chem. Eng. Sci.* 166, 66–76. <https://doi.org/10.1016/j.ces.2017.03.027>.
- Li, L., Wu, H., Chen, H., Zhang, J., Xu, X., Wang, Shuaijun, Wang, Shaobin, Sun, H., 2020. Heterogeneous activation of peroxymonosulfate by hierarchically porous cobalt/iron bimetallic oxide nanosheets for degradation of phenol solutions. *Chemosphere* 256, 127160. <https://doi.org/10.1016/j.chemosphere.2020.127160>.
- Li, X., Liu, W., Ma, J., Wen, Y., Wu, Z., 2015. High catalytic activity of magnetic Fe₃O₄/NiO_y/SBA-15: the role of Ni in the bimetallic oxides at the nanometer level. *Appl. Catal. B Environ.* 179, 239–248. <https://doi.org/10.1016/j.apcatb.2015.05.034>.
- Li, Y., Jawad, A., Khan, A., Lu, X., Chen, Z., Liu, W., Yin, G., 2016. Synergistic degradation of phenols by bimetallic CuO-Co₃O₄@γ-Al₂O₃ catalyst in H₂O₂/HCO₃-system. *Cuihua Xuebao/Chinese J. Catal.* 37, 963–970. [https://doi.org/10.1016/S1872-2067\(15\)61092-0](https://doi.org/10.1016/S1872-2067(15)61092-0).
- Liao, F., Lo, T.W.B., Tsang, S.C.E., 2015. Recent developments in palladium-based bimetallic catalysts. *ChemCatChem* 7, 1998–2014. <https://doi.org/10.1002/cctc.201500245>.
- Liotta, L.F., Gruttadauria, M., Di Carlo, G., Perrini, G., Librando, V., 2009. Heterogeneous catalytic degradation of phenolic substrates: catalysts activity. *J. Hazard Mater.* 162, 588–606. <https://doi.org/10.1016/j.jhazmat.2008.05.115>.
- Liu, C.J., Vissokov, G.P., Jang, B.W.L., 2002. Catalyst preparation using plasma technologies. *Catal. Today* 72, 173–184. [https://doi.org/10.1016/S0920-5861\(01\)00491-6](https://doi.org/10.1016/S0920-5861(01)00491-6).
- Liu, X., Chen, Zhengxian, Chen, Zuliang, Megharaj, M., Naidu, R., 2013. Remediation of Direct Black G in wastewater using kaolin-supported bimetallic Fe/Ni nanoparticles. *Chem. Eng. J.* 223, 764–771. <https://doi.org/10.1016/j.cej.2013.03.002>.
- Louis, C., 2016. Chemical preparation of supported bimetallic catalysts. Gold-based bimetallic, a case study. *Catalysts* 6. <https://doi.org/10.3390/catal6080110>.
- Ma, Y., Hu, K., Sun, Y., Iqbal, K., Bai, Z., Wang, C., Jia, X., Ye, W., 2019. N-doped carbon coated Mn₃O₄/PdCu nanocomposite as a high-performance catalyst for 4-nitrophenol reduction. *Sci. Total Environ.* 696, 134013. <https://doi.org/10.1016/j.scitotenv.2019.134013>.
- Marchesini, F.A., Aghemo, V., Moreno, I., Navascués, N., Irusta, S., Gutierrez, L., 2020. Journal of Environmental Chemical Engineering Pd and Pt, in nanoparticles supported on polymer fibres as catalysts for the nitrate and nitrite reduction in aqueous media. *J. Environ. Chem. Eng.* 8, 103651. <https://doi.org/10.1016/j.jece.2019.103651>.
- Mohd Zabidi, N.A., Abdul Aziz, M.N.A., Ali, S., Taha, M.F., 2012. Synthesis and characterization of Fe-Co catalyst prepared via reverse microemulsion method. *AIP Conf. Proc.* 1482, 590–594. <https://doi.org/10.1063/1.4757540>.
- Mok, Y.S., Kim, D.H., 2011. Treatment of toluene by using adsorption and

- nonthermal plasma oxidation process. *Curr. Appl. Phys.* 11, S58–S62. <https://doi.org/10.1016/j.cap.2011.05.023>.
- Munnik, P., De Jongh, P.E., De Jong, K.P., 2015. Recent developments in the synthesis of supported catalysts. *Chem. Rev.* 115, 6687–6718. <https://doi.org/10.1021/cr500486u>.
- Munoz, M., de Pedro, Z.M., Casas, J.A., Rodriguez, J.J., 2014. Improved Γ -alumina-supported Pd and Rh catalysts for hydrodechlorination of chlorophenols. *Appl. Catal. Gen.* 488, 78–85. <https://doi.org/10.1016/j.apcata.2014.09.035>.
- Munoz, M., de Pedro, Z.M., Casas, J.A., Rodriguez, J.J., 2013. Chlorophenols breakdown by a sequential hydrodechlorination-oxidation treatment with a magnetic Pd-Fe γ -Al₂O₃ catalyst. *Water Res.* 47, 3070–3080. <https://doi.org/10.1016/j.watres.2013.03.024>.
- Neyts, E.C., 2016. Plasma-surface interactions in plasma catalysis. *Plasma Chem. Plasma Process.* 36, 185–212. <https://doi.org/10.1007/s11090-015-9662-5>.
- Nguyen, H.-T.T., Dinh, V.-P., Phan, Q.-A.N., Tran, V.A., Doan, V.-D., Lee, T., Nguyen, T.D., 2020. Bimetallic Al/Fe Metal-Organic Framework for highly efficient photo-Fenton degradation of rhodamine B under visible light irradiation. *Mater. Lett.* 279, 128482. <https://doi.org/10.1016/j.matlet.2020.128482>.
- Nutt, M.O., Heck, K.N., Alvarez, P., Wong, M.S., 2006. Improved Pd-on-Au bimetallic nanoparticle catalysts for aqueous-phase trichloroethene hydrodechlorination. *Appl. Catal. B Environ.* 69, 115–125. <https://doi.org/10.1016/j.apcatb.2006.06.005>.
- Oruc, Z., Ergüt, M., Uzunoğlu, D., Özer, A., 2019. Green synthesis of biomass-derived activated carbon/Fe-Zn bimetallic nanoparticles from lemon (*Citrus limon* (L.) Burm. f.) wastes for heterogeneous Fenton-like decolorization of Reactive Red 2. *J. Environ. Chem. Eng.* 7 <https://doi.org/10.1016/j.jece.2019.103231>.
- Ou, J.H., Sheu, Y.T., Tsang, D.C.W., Sun, Y.J., Kao, C.M., 2020. Application of iron/aluminum bimetallic nanoparticle system for chromium-contaminated groundwater remediation. *Chemosphere* 256, 127158. <https://doi.org/10.1016/j.chemosphere.2020.127158>.
- Palomares, A.E., Franch, C., Corma, A., 2011. A study of different supports for the catalytic reduction of nitrates from natural water with a continuous reactor. *Catal. Today* 172, 90–94. <https://doi.org/10.1016/j.cattod.2011.05.015>.
- Pandya, A., Pandya, C., Dave, B., 2018. *International Journal of Advance Engineering and Research BIODEGRADATION OF TOXIC DYES AND TEXTILE DYE EFFLUENT – A REVIEW 1246–1249*.
- Park, J., Hwang, Y., Bae, S., 2019. Nitrate reduction on surface of Pd/Sn catalysts supported by coal fly ash-derived zeolites. *J. Hazard Mater.* 374, 309–318. <https://doi.org/10.1016/j.jhazmat.2019.04.051>.
- Patnaik, S., Sahoo, D.P., Parida, K.M., 2020. Bimetallic co-effect of Au-Pd alloyed nanoparticles on mesoporous silica modified g-C₃N₄ for single and simultaneous photocatalytic oxidation of phenol and reduction of hexavalent chromium. *J. Colloid Interface Sci.* 560, 519–535. <https://doi.org/10.1016/j.jcis.2019.09.041>.
- Perego, C., Villa, P., 1997. Catalyst preparation methods. *Catal. Today* 34, 281–305. [https://doi.org/10.1016/S0920-5861\(96\)00055-7](https://doi.org/10.1016/S0920-5861(96)00055-7).
- Pheleps, T.J., Niedzielski, J.J., Malachowsky, K.J., Schram, R.M., Herbes, S.E., White, D.C., 1991. Biodegradation of mixed-organic wastes by microbial consortia in continuous-recycle expanded-bed bioreactors. *Environ. Sci. Technol.* 25, 1461–1465. <https://doi.org/10.1021/es00020a015>.
- Pinna, F., 1998. Supported metal catalysts preparation. *Catal. Today* 41, 129–137. [https://doi.org/10.1016/S0920-5861\(98\)00043-1](https://doi.org/10.1016/S0920-5861(98)00043-1).
- Pintar, A., Setinc, M., Levec, J., 1998. Hardness and salt effects on catalytic hydrogenation of aqueous nitrate solutions. *J. Catal.* 174, 72–87. <https://doi.org/10.1006/jcat.1997.1960>.
- Pizarro, A.H., Molina, C.B., Rodriguez, J.J., Epron, F., 2015. Catalytic reduction of nitrate and nitrite with mono- and bimetallic catalysts supported on pillared clays. *J. Environ. Chem. Eng.* 3, 2777–2785. <https://doi.org/10.1016/j.jece.2015.09.026>.
- Pradhan, A.C., Sahoo, M.K., Bellamkonda, S., Parida, K.M., Rao, G.R., 2016. Enhanced photodegradation of dyes and mixed dyes by heterogeneous mesoporous Co-Fe/Al₂O₃-MCM-41 nanocomposites: nanoparticles formation, semiconductor behavior and mesoporosity. *RSC Adv.* 6, 94263–94277. <https://doi.org/10.1039/c6ra19923b>.
- Puliyalil, H., Lasić Jurković, D., Dasireddy, V.D.B.C., Likozar, B., 2018. A review of plasma-assisted catalytic conversion of gaseous carbon dioxide and methane into value-added platform chemicals and fuels. *RSC Adv.* 8, 27481–27508. <https://doi.org/10.1039/c8ra03146k>.
- Quito, K.G., Doma, B., Futralan, C.M., Wan, M.W., 2018. Removal of chromium(VI) and zinc(II) from aqueous solution using kaolin-supported bacterial biofilms of Gram-negative *E. coli* and Gram-positive *Staphylococcus epidermidis*. *Sustain. Environ. Res.* 28, 206–213. <https://doi.org/10.1016/j.serj.2018.04.002>.
- Rani, M., Shanker, U., 2018. Photocatalytic degradation of toxic phenols from water using bimetallic metal oxide nanostructures. *Colloids Surfaces A Physicochem. Eng. Asp.* 553, 546–561. <https://doi.org/10.1016/j.colsurfa.2018.05.071>.
- Riaz, N., Bustam, M.A., Chong, F.K., Man, Z.B., Khan, M.S., Shariff, A.M., 2014. Photocatalytic degradation of DIPA using bimetallic Cu-Ni/TiO₂ photocatalyst under visible light irradiation. *Sci. World J.* <https://doi.org/10.1155/2014/342020>.
- Riaz, N., Dutta, B.K., Khan, M.S., Nurlaela, E., Dhobi, A., 2012. Photocatalytic degradation of orange II using bimetallic Cu-Ni/TiO₂ photocatalysts 1, pp. 1–5.
- Rida, K., López Cámara, A., Peña, M.A., Bolívar-Díaz, C.L., Martínez-Arias, A., 2014. Bimetallic Co-Fe and Co-Cr oxide systems supported on CeO₂: characterization and CO oxidation catalytic behaviour. *Int. J. Hydrogen Energy* 40, 11267–11278. <https://doi.org/10.1016/j.ijhydene.2015.03.044>.
- Rodrigues, C.S.D., Silva, R.M., Carabineiro, S.A.C., Maldonado-Hódar, F.J., Madeira, L.M., 2019. Wastewater treatment by catalytic wet peroxidation using nano gold-based catalysts: a review. *Catalysts* 9. <https://doi.org/10.3390/catal9050478>.
- Sá, J., Vinek, H., 2005. Catalytic hydrogenation of nitrates in water over a bimetallic catalyst. *Appl. Catal. B Environ.* 57, 247–256. <https://doi.org/10.1016/j.apcatb.2004.10.019>.
- Sandoval, A., Aguilar, A., Louis, C., Traverse, A., Zanella, R., 2011. Bimetallic Au-Ag/TiO₂ catalyst prepared by deposition-precipitation: high activity and stability in CO oxidation. *J. Catal.* 281, 40–49. <https://doi.org/10.1016/j.jcat.2011.04.003>.
- Sandoval, A., Louis, C., Zanella, R., 2013. Improved activity and stability in CO oxidation of bimetallic Au-Cu/TiO₂ catalysts prepared by deposition-precipitation with urea. *Appl. Catal. B Environ.* 140–141, 363–377. <https://doi.org/10.1016/j.apcatb.2013.04.039>.
- Shen, C., Li, H., Wen, Y., Zhao, F., Zhang, Y., Wu, D., Liu, Y., Li, F., 2020. Spherical Cu₂O-Fe₃O₄/chitosan bifunctional catalyst for coupled Cr-organic complex oxidation and Cr(VI) capture-reduction. *Chem. Eng. J.* 383, 123105. <https://doi.org/10.1016/j.cej.2019.123105>.
- Shi, D., Ouyang, Z., Zhao, Y., Xiong, J., Shi, X., 2019. Catalytic reduction of hexavalent chromium using iron/palladium bimetallic nanoparticle-assembled filter paper. *Nanomaterials* 9. <https://doi.org/10.3390/nano9081183>.
- Sierra-Salazar, A.F., Ayrál, A., Chave, T., Hulea, V., Nikitenko, S.I., Abate, S., Perathoner, S., Lacroix-Desmazes, P., 2019. Unconventional pathways for designing silica-supported Pt and Pd catalysts with hierarchical porosity. *Stud. Surf. Sci. Catal.* 178, 377–397. <https://doi.org/10.1016/B978-0-444-64127-4.00018-5>.
- Silas, K., Ghani, W.A.W.A.K., Choong, T.S.Y., Rashid, U., 2018. Breakthrough studies of Co₃O₄ supported activated carbon monolith for simultaneous SO₂/NO_x removal from flue gas. *Fuel Process. Technol.* 180, 155–165. <https://doi.org/10.1016/j.fuproc.2018.08.018>.
- Singh, K.P., Singh, A.K., Gupta, S., Sinha, S., 2011. Optimization of Cr(VI) reduction by zero-valent bimetallic nanoparticles using the response surface modeling approach. *Desalination* 270, 275–284. <https://doi.org/10.1016/j.desal.2010.11.056>.
- Soares, O.S.G.P., Marques, L., Freitas, C.M.A.S., Fonseca, A.M., Parpot, P., Órfão, J.J.M., Pereira, M.F.R., Neves, I.C., 2015. Mono and bimetallic NaY catalysts with high performance in nitrate reduction in water. *Chem. Eng. J.* 281, 411–417. <https://doi.org/10.1016/j.cej.2015.06.093>.
- Soares, O.S.G.P., Órfão, J.J.M., Pereira, M.F.R., 2011. Nitrate reduction in water catalysed by Pd-Cu on different supports. *Desalination* 279, 367–374. <https://doi.org/10.1016/j.desal.2011.06.037>.
- Soares, O.S.G.P., Órfão, J.J.M., Pereira, M.F.R., 2009. Bimetallic catalysts supported on activated carbon for the nitrate reduction in water: optimization of catalysts composition. *Appl. Catal. B Environ.* 91, 441–448. <https://doi.org/10.1016/j.apcatb.2009.06.013>.
- Soares, O.S.G.P., Órfão, J.J.M., Ruiz-Martínez, J., Silvestre-Albergo, J., Sepúlveda-Escribano, A., Pereira, M.F.R., 2010. Pd-Cu/AC and Pt-Cu/AC catalysts for nitrate reduction with hydrogen: influence of calcination and reduction temperatures. *Chem. Eng. J.* 165, 78–88. <https://doi.org/10.1016/j.cej.2010.08.065>.
- Strandberg, G.W., Donaldson, T.L., Farr, L.L., 1989. Degradation of trichloroethylene and trans-1,2-dichloroethylene by a methanotrophic consortium in a fixed-film, packed-bed bioreactor. *Environ. Sci. Technol.* 23, 1422–1425. <https://doi.org/10.1021/es00069a016>.
- Su, J., Lin, S., Chen, Z., Megharaj, M., Naidu, R., 2011. Dechlorination of p-chlorophenol from aqueous solution using bentonite supported Fe/Pd nanoparticles: synthesis, characterization and kinetics. *Desalination* 280, 167–173. <https://doi.org/10.1016/j.desal.2011.06.067>.
- Sun, H., Abdeta, A.B., Zelekew, O.A., Guo, Y., Zhang, J., Kuo, D.H., Lin, J., Chen, X., 2020. Spherical porous SiO₂ supported CuVOS catalyst with an efficient catalytic reduction of pollutants under dark condition. *J. Mol. Liq.* 313, 113567. <https://doi.org/10.1016/j.molliq.2020.113567>.
- Sun, Q., Liu, M., Li, K., Han, Y., Zuo, Y., Chai, F., Song, C., Zhang, G., Guo, X., 2017. Synthesis of Fe/M (M = Mn, Co, Ni) bimetallic metal organic frameworks and their catalytic activity for phenol degradation under mild conditions. *Inorg. Chem. Front.* 4, 144–153. <https://doi.org/10.1039/c6qi00441e>.
- Sun, X., Xu, D., Dai, P., Liu, X., Tan, F., Guo, Q., 2020. Efficient degradation of methyl orange in water via both radical and non-radical pathways using Fe-Co bimetal-doped MCM-41 as peroxymonosulfate activator. *Chem. Eng. J.* 402, 125881. <https://doi.org/10.1016/j.cej.2020.125881>.
- Taghavimoghaddam, J., Knowles, G.P., Chaffee, A.L., 2012. Preparation and characterization of mesoporous silica supported cobalt oxide as a catalyst for the oxidation of cyclohexanol. *J. Mol. Catal. Chem.* 358, 79–88. <https://doi.org/10.1016/j.molcata.2012.02.014>.
- Tang, S., Yuan, D., Zhang, Q., Liu, Y., Zhang, Q., Liu, Z., Huang, H., 2016. Fe-Mn bimetallic oxides loaded on granular activated carbon to enhance dye removal by catalytic ozonation. *Environ. Sci. Pollut. Res.* 23, 18800–18808. <https://doi.org/10.1007/s11356-016-7030-5>.
- Tao, F., Zhang, S., Luan, N., Zhang, X., 2012. Action of bimetallic nanocatalysts under reaction conditions and during catalysis: evolution of chemistry from high vacuum conditions to reaction conditions. *Chem. Soc. Rev.* 41, 7980–7993. <https://doi.org/10.1039/c2cs35185d>.
- Tran, K.Y., Heinrichs, B., Colomer, J.F., Pirard, J.P., Lambert, S., 2007. Carbon nanotubes synthesis by the ethylene chemical catalytic vapour deposition (CCVD) process on Fe, Co, and Fe-Co/Al₂O₃ sol-gel catalysts. *Appl. Catal. Gen.* 318, 63–69. <https://doi.org/10.1016/j.apcata.2006.10.042>.
- Trapido, M., Veressina, Y., Munter, R., 1998. Advanced oxidation processes for

- degradation of 2,4-dichloro- and 2,4-dimethylphenol. *J. Environ. Eng.* 124, 690–694. [https://doi.org/10.1061/\(ASCE\)0733-9372](https://doi.org/10.1061/(ASCE)0733-9372).
- Trawczyński, J., Gheek, P., Okal, J., Zawadzki, M., Gomez, M.J.I., 2011. Reduction of nitrate on active carbon supported Pd-Cu catalysts. *Appl. Catal. A Gen.* 409–410, 39–47. <https://doi.org/10.1016/j.apcata.2011.09.020>.
- Tütem, E., Apak, R., Ünal, Ç.F., 1998. Adsorptive removal of chlorophenols from water by bituminous shale. *Water Res.* 32, 2315–2324. [https://doi.org/10.1016/S0043-1354\(97\)00476-4](https://doi.org/10.1016/S0043-1354(97)00476-4).
- Uskoković, V., Drogenik, M., 2005. Synthesis of materials within reverse micelles. *Surf. Rev. Lett.* 12, 239–277. <https://doi.org/10.1142/S0218625X05007001>.
- Van Der Lee, M.K., Van Jos Dillen, A., Bitter, J.H., De Jong, K.P., 2005. Deposition precipitation for the preparation of carbon nanofiber supported nickel catalysts. *J. Am. Chem. Soc.* 127, 13573–13582. <https://doi.org/10.1021/ja053038q>.
- Vilela, P.B., Dalalibera, A., Duminelli, E.C., Becegato, V.A., Paulino, A.T., 2019. Adsorption and removal of chromium (VI) contained in aqueous solutions using a chitosan-based hydrogel. *Environ. Sci. Pollut. Res.* 26, 28481–28489. <https://doi.org/10.1007/s11356-018-3208-3>.
- Villegas, L.G.C., Mashhadi, N., Chen, M., Mukherjee, D., Taylor, K.E., Biswas, N., 2016. A short review of techniques for phenol removal from wastewater. *Curr. Pollut. Reports* 2, 157–167. <https://doi.org/10.1007/s40726-016-0035-3>.
- Vinotha Alex, A., Chandrasekaran, N., Mukherjee, A., 2020. Novel enzymatic synthesis of core/shell AgNP/AuNC bimetallic nanostructure and its catalytic applications. *J. Mol. Liq.* 301, 112463. <https://doi.org/10.1016/j.molliq.2020.112463>.
- Wada, K., Hirata, T., Hosokawa, S., Iwamoto, S., Inoue, M., 2012. Effect of supports on Pd-Cu bimetallic catalysts for nitrate and nitrite reduction in water. *Catal. Today* 185, 81–87. <https://doi.org/10.1016/j.cattod.2011.07.021>.
- Wali, L.A., Alwan, A.M., Dheyab, A.B., Hashim, D.A., 2019. Excellent fabrication of Pd-Ag NPs/PSI photocatalyst based on bimetallic nanoparticles for improving methylene blue photocatalytic degradation. *Optik* 179, 708–717. <https://doi.org/10.1016/j.ijleo.2018.11.011>.
- Wang, J., Liu, C., Feng, J., Cheng, D., Zhang, C., Yao, Y., Gu, Z., Hu, W., Wan, J., Yu, C., 2020. MOFs derived Co/Cu bimetallic nanoparticles embedded in graphitized carbon nanocubes as efficient Fenton catalysts. *J. Hazard Mater.* 394, 122567. <https://doi.org/10.1016/j.jhazmat.2020.122567>.
- Wang, J., Liu, C., Hussain, I., Li, C., Li, J., Sun, X., Shen, J., 2016. RSC Advances hollow mesoporous silica spheres : the effect of Fe/Cu ratio on heterogeneous Fenton degradation of 54623–54635. <https://doi.org/10.1039/c6ra08501f>.
- Wang, J., Liu, C., Li, J., Luo, R., Hu, X., Sun, X., Shen, J., Han, W., Wang, L., 2017. In-situ incorporation of iron-copper bimetallic particles in electropun carbon nanofibers as an efficient Fenton catalyst. *Appl. Catal. B Environ.* 207, 316–325. <https://doi.org/10.1016/j.apcatb.2017.02.032>.
- Wang, J., Liu, C., Tong, L., Li, J., Luo, R., Qi, J., Li, Y., Wang, L., 2015. Iron-copper bimetallic nanoparticles supported on hollow mesoporous silica spheres: an effective heterogeneous Fenton catalyst for orange II degradation. *RSC Adv.* 5, 69593–69605. <https://doi.org/10.1039/c5ra10826h>.
- Wang, P., Liang, Y.N., Zhong, Z., Hu, X., 2020. Nano-hybrid bimetallic Au-Pd catalysts for ambient condition-catalytic wet air oxidation (AC-CWAO) of organic dyes. *Separ. Purif. Technol.* 233, 115960. <https://doi.org/10.1016/j.seppur.2019.115960>.
- Wang, S., Meng, F., Sun, X., Bao, M., Ren, J., Yu, S., Zhang, Z., Ke, J., Zeng, L., 2020. Bimetallic Fe/In metal-organic frameworks boosting charge transfer for enhancing pollutant degradation in wastewater. *Appl. Surf. Sci.* 528, 147053. <https://doi.org/10.1016/j.apsusc.2020.147053>.
- Wang, X., Chen, C., Chang, Y., Liu, H., 2009. Dechlorination of chlorinated methanes by Pd/Fe bimetallic nanoparticles. *J. Hazard Mater.* 161, 815–823. <https://doi.org/10.1016/j.jhazmat.2008.04.027>.
- Wang, X., Chen, C., Liu, H., Ma, J., 2008. Characterization and evaluation of catalytic dechlorination activity of Pd/Fe bimetallic nanoparticles. *Ind. Eng. Chem. Res.* 47, 8645–8651. <https://doi.org/10.1021/ie701762d>.
- Wang, Y., Li, Q., Zhang, P., O'Connor, D., Varma, R.S., Yu, M., Hou, D., 2019. One-pot green synthesis of bimetallic hollow palladium-platinum nanotubes for enhanced catalytic reduction of p-nitrophenol. *J. Colloid Interface Sci.* 539, 161–167. <https://doi.org/10.1016/j.jcis.2018.12.053>.
- Wei, J., Xu, X., Liu, Y., Wang, D., 2006. Catalytic hydrodechlorination of 2,4-dichlorophenol over nanoscale Pd/Fe: reaction pathway and some experimental parameters. *Water Res.* 40, 348–354. <https://doi.org/10.1016/j.watres.2005.10.017>.
- Wei, Z.S., Li, H.Q., He, J.C., Ye, Q.H., Huang, Q.R., Luo, Y.W., 2013. Removal of dimethyl sulfide by the combination of non-thermal plasma and biological process. *Bioresour. Technol.* 146, 451–456. <https://doi.org/10.1016/j.biortech.2013.07.114>.
- Witońska, I.A., Walock, M.J., Binczarski, M., Lesiak, M., Stanishevsky, A.V., Karski, S., 2014. Pd-Fe/SiO₂ and Pd-Fe/Al₂O₃ catalysts for selective hydrodechlorination of 2,4-dichlorophenol into phenol. *J. Mol. Catal. Chem.* 393, 248–256. <https://doi.org/10.1016/j.molcata.2014.06.022>.
- Wu, J.M., Wen, W., 2010. Catalyzed degradation of azo dyes under ambient conditions. *Environ. Sci. Technol.* 44, 9123–9127. <https://doi.org/10.1021/es1027234>.
- Wu, Q., Siddique, M.S., Yu, W., 2021. Iron-nickel bimetallic metal-organic frameworks as bifunctional Fenton-like catalysts for enhanced adsorption and degradation of organic contaminants under visible light: kinetics and mechanistic studies. *J. Hazard Mater.* 401, 123261. <https://doi.org/10.1016/j.jhazmat.2020.123261>.
- Xia, M., Long, M., Yang, Y., Chen, C., Cai, W., Zhou, B., 2011. A highly active bimetallic oxides catalyst supported on Al-containing MCM-41 for Fenton oxidation of phenol solution. *Appl. Catal. B Environ.* 110, 118–125. <https://doi.org/10.1016/j.apcatb.2011.08.033>.
- Xu, L., Zhao, L., Mao, Y., Zhou, Z., Wu, D., 2020. Enhancing the degradation of bisphenol A by dioxygen activation using bimetallic Cu/Fe:zeolite: critical role of Cu(I) and superoxide radical. *Separ. Purif. Technol.* 253, 117550. <https://doi.org/10.1016/j.seppur.2020.117550>.
- Xu, X., Zhou, H., He, P., Wang, D., 2005a. Catalytic dechlorination kinetics of p-dichlorobenzene over Pd/Fe catalysts. *Chemosphere* 58, 1135–1140. <https://doi.org/10.1016/j.chemosphere.2004.07.010>.
- Xu, X., Zhou, M., He, P., Hao, Z., 2005b. Catalytic reduction of chlorinated and recalcitrant compounds in contaminated water. *J. Hazard Mater.* 123, 89–93. <https://doi.org/10.1016/j.jhazmat.2005.04.002>.
- Yan, Q., Wang, X., Feng, J., Mei, L., Wang, A., 2020. Simple fabrication of bimetallic platinum-rhodium alloyed nano-multipods : a highly effective and recyclable catalyst for reduction of 4-nitrophenol and rhodamine B. *J. Colloid Interface Sci.* <https://doi.org/10.1016/j.jcis.2020.08.062>.
- Yan, X., Yue, D., Guo, C., Wang, S., Qian, X., Zhao, Y., 2020. Effective removal of chlorinated organic pollutants by bimetallic iron-nickel sulfide activation of peroxydisulfate. *Chin. Chem. Lett.* 31, 1535–1539. <https://doi.org/10.1016/j.ccllet.2019.11.003>.
- Yang, Z., Zhang, X., Pu, S., Ni, R., Lin, Y., Liu, Y., 2019. Novel Fenton-like system (Mg/Fe-O₂) for degradation of 4-chlorophenol. *Environ. Pollut.* 250, 906–913. <https://doi.org/10.1016/j.envpol.2019.04.096>.
- Yao, Y., Zhang, J., Chen, H., Yu, M., Gao, M., Hu, Y., Wang, S., 2018. Ni 0 encapsulated in N-doped carbon nanotubes for catalytic reduction of highly toxic hexavalent chromium. *Appl. Surf. Sci.* 440, 421–431. <https://doi.org/10.1016/j.apsusc.2018.01.123>.
- Yip, A.C.K., Leung-Yuk Lam, F., Hu, X., 2007. Novel bimetallic catalyst for the photo-assisted degradation of Acid Black 1 over a broad range of pH. *Chem. Eng. Sci.* 62, 5150–5153. <https://doi.org/10.1016/j.ces.2007.01.014>.
- Yoshinaga, Y., Akita, T., Mikami, I., Okuhara, T., 2002. Hydrogenation of nitrate in water to nitrogen over Pd-Cu supported on active carbon. *J. Catal.* 207, 37–45. <https://doi.org/10.1006/jcat.2002.3529>.
- Yu, W., Porosoff, M.D., Chen, J.C., 2012. Review of Pt-based bimetallic catalysis: from model surfaces to supported catalysts. *Chem. Rev.* 112, 5780–5817. <https://doi.org/10.1021/cr300096b>.
- Yuan, D., Gong, X., Wu, R., 2007. Ensemble effects on ethylene dehydrogenation on PdAu(001) surfaces investigated with first-principles calculations and nudged-elastic-band simulations. *Phys. Rev. B Condens. Matter* 75, 3–6. <https://doi.org/10.1103/PhysRevB.75.233401>.
- Yuan, Y., Li, H., Lai, B., Yang, P., Gou, M., Zhou, Y., Sun, G., 2014. Removal of high-concentration Cl⁻ acid orange 7 from aqueous solution by zerovalent iron/copper (Fe/Cu) bimetallic particles. *Ind. Eng. Chem. Res.* 53, 2605–2613. <https://doi.org/10.1021/ie402739s>.
- Zekeew, O.A., Kuo, D.H., Abdullah, H., 2019. Synthesis of (Sn,Zn)(O,S) bimetallic oxysulfide catalyst for the detoxification of Cr⁺⁶ in aqueous solution. *Adv. Powder Technol.* 30, 3099–3106. <https://doi.org/10.1016/j.apt.2019.09.016>.
- Zhang, S.S., Yang, N., Zhuang, X., Ren, L., Natarajan, V., Cui, Z., Si, H., Xin, X., Ni, S.Q., Zhan, J., 2019. Montmorillonite immobilized Fe/Ni bimetallic prepared by dry in-situ hydrogen reduction for the degradation of 4-Chlorophenol. *Sci. Rep.* 9, 1–9. <https://doi.org/10.1038/s41598-019-49349-w>.
- Zhang, W., Zhang, H., Yan, X., Zhang, M., Luo, R., Qi, J., Sun, X., Shen, J., Han, W., Wang, L., Li, J., 2020. Controlled synthesis of bimetallic Prussian blue analogues to activate peroxymonosulfate for efficient bisphenol A degradation. *J. Hazard Mater.* 387, 121701. <https://doi.org/10.1016/j.jhazmat.2019.121701>.
- Zhang, Y., Park, S.J., 2019. Stabilization of dispersed CuPd bimetallic alloy nanoparticles on ZIF-8 for photoreduction of Cr(VI) in aqueous solution. *Chem. Eng. J.* 369, 353–362. <https://doi.org/10.1016/j.cej.2019.03.083>.
- Zhang, Z., Shen, Q., Cissoko, N., Wo, J., Xu, X., 2010. Catalytic dechlorination of 2,4-dichlorophenol by Pd/Fe bimetallic nanoparticles in the presence of humic acid. *J. Hazard Mater.* 182, 252–258. <https://doi.org/10.1016/j.jhazmat.2010.06.022>.
- Zhao, M., Church, T.L., Harris, A.T., 2011. SBA-15 supported Ni-Co bimetallic catalysts for enhanced hydrogen production during cellulose decomposition. *Appl. Catal. B Environ.* 101, 522–530. <https://doi.org/10.1016/j.apcatb.2010.10.024>.
- Zhou, S., Li, Y., Chen, J., Liu, Z., Wang, Z., Na, P., 2014. Enhanced Cr(VI) removal from aqueous solutions using Ni/Fe bimetallic nanoparticles: characterization, kinetics and mechanism. *RSC Adv.* 4, 50699–50707. <https://doi.org/10.1039/c4ra08754b>.
- Zhou, X., Jing, G., Lv, B., Zhou, Z., Zhu, R., 2016. Highly efficient removal of chromium(VI) by Fe/Ni bimetallic nanoparticles in an ultrasound-assisted system. *Chemosphere* 160, 332–341. <https://doi.org/10.1016/j.chemosphere.2016.06.103>.
- Zhou, Y., Kuang, Y., Li, W., Chen, Z., Megharaj, M., Naidu, R., 2013. A combination of bentonite-supported bimetallic Fe/Pd nanoparticles and biodegradation for the remediation of p-chlorophenol in wastewater. *Chem. Eng. J.* 223, 68–75. <https://doi.org/10.1016/j.cej.2013.02.118>.